AD_____

Award Number: DAMD17-02-1-0321

TITLE: Induction of Apoptosis by Targeting the Microtubule Network: Using HIV Tat as a Model System

PRINCIPAL INVESTIGATOR: Dan Chen
Dr. Qiang Zhou

CONTRACTING ORGANIZATION: University of California
Berkeley, CA 94720-5940

REPORT DATE: April 2004

TYPE OF REPORT: Annual Summary

PREPARED FOR: U.S. Army Medical Research and Materiel Command
Fort Detrick, Maryland 21702-5012

REPORT DOCUMENTATION PAGE

Form Approved
OMB No. 074-0188

1. AGENCY USE ONLY (Leave blank)	2. REPORT DATE	3. REPORT TYPE AND DATES COVERED
	April 2004	Annual Summary (18 Mar 2003 - 17 Mar 2004)

4. TITLE AND SUBTITLE

Induction of Apoptosis by Targeting the Microtubule Network: Using HIV Tat as a Model System

5. FUNDING NUMBERS

DAMD17-02-1-0321

6. AUTHOR(S)

Dan Chen
Dr. Qiang Zhou

7. PERFORMING ORGANIZATION NAME(S) AND ADDRESS(ES)

University of California
Berkeley, CA 94720-5940

E-Mail: chendan@uclink4.berkeley.edu

8. PERFORMING ORGANIZATION REPORT NUMBER

9. SPONSORING / MONITORING AGENCY NAME(S) AND ADDRESS(ES)

U.S. Army Medical Research and Materiel Command
Fort Detrick, Maryland 21702-5012

10. SPONSORING / MONITORING AGENCY REPORT NUMBER

11. SUPPLEMENTARY NOTES

12a. DISTRIBUTION / AVAILABILITY STATEMENT

Approved for Public Release; Distribution Unlimited

12b. DISTRIBUTION CODE

13. ABSTRACT (Maximum 200 Words)

Not Provided

14. SUBJECT TERMS

Not Provided

15. NUMBER OF PAGES

21

16. PRICE CODE

17. SECURITY CLASSIFICATION OF REPORT	18. SECURITY CLASSIFICATION OF THIS PAGE	19. SECURITY CLASSIFICATION OF ABSTRACT	20. LIMITATION OF ABSTRACT
Unclassified	Unclassified	Unclassified	Unlimited

Table of Contents

Final Annual Summary Report

Dan Chen

HIV-1 Tat is absolutely essential for HIV replication and has been shown to have many functions. I started my graduate work with the characterization of Tat-induced apoptosis, which contributes in part to the progressive CD4+ T cell loss in AIDS patients. Based on my previous data, we proposed a model by which Tat induces apoptosis in T cells. Tat interacts with tubulin and polymerized microtubules, leading to the alteration of microtubule dynamics and the activation of a mitochondria-dependent apoptotic pathway. Bim, a pro-apoptotic Bcl-2 relative and a transducer of death signals initiated by perturbation of microtubule dynamics, facilitates Tat-induced apoptosis. This work has been published in EMBO Journal.

Next, I addressed how Bim tranduces the Tat-induced apoptotic signals in T cells. Bim is a proapoptotic Bcl-2 family member, exerting its apoptotic activity by antagonizing the anti-apoptotic Bcl-2 family members. There are three forms of Bim due to alternative splicing: BimEL, BimL and BimS. The expression of different forms of Bim varies in different cell types. Bim knockout mice demonstrated severe perturbation of the development of lymph system. Furthermore, Bim and Bcl-2 double knockout prevented all the disorders caused by Bcl-2 deficiency. Thus, the activity of Bim, a major antagonist of Bcl-2, plays an important role in regulating the programmed cell death in lymphocytes.

My study demonstrated that BimEL is the dominant form expressed in T cells, which is sequestered to microtubules through a direct interaction with tubulin and kept away from its targets, the anti-apoptotic Bcl-2 family members, in the mitochondria. Phosphorylation releases BimEL from microtubules, and the freed BimEL translocates to its battlefield, the mitochondria. However, it is still not fully active due to its poor interaction with Bcl-2. Only after the freed BimEL is cleaved by caspases to increase its interaction with Bcl-2, is it fully activated. Apoptosis is triggered when BH3-only proteins of the Bcl-2 family are activated and block the anti-apoptotic activities of Bcl-2. Thus, the activation of BimEL, an initiator of apoptosis, downstream of the caspase cascade provides a positive feedback control during apoptosis.

To test the hypothesis that phosphorylated BimEL is released from microtubules and becomes more accessible for caspase cleavage, I treated Jurkat cells with Okadaic Acid (OA), a phosphotase inhibitor, which completely converted unphosphorylated BimEL to the phosphorylated form. The subsequent separation of the microtubule fraction from the soluble fraction and the detection of BimEL associated with microtubules showed that all BimEL dissociated from microtubules in OA treated cell lysates. Furthermore, in cells treated with apoptosis inducer staurosporine, only phosphorylated BimEL was dissociated from microtubules and got cleaved during apoptosis, suggesting that this model also holds in vivo.

A time course analysis of the cleavage of BimEL demonstrated that the cleavage event occurred 1 hour after Stuarosporine treatment, when only less than 6% of cells were

undergoing apoptosis. This suggested that the cleavage of BimEL happened at a very early stage of apoptosis, and might contribute to the progression of cell death.

This model is derived from studies in Jurkat T cell line treated with apoptosis stimuli, such as staurosporine, UV and TNF, therefore the generality of this model need to be tested. The same phenomenon was also observed in mouse activated primary T lymphocytes, but not in immature T cell lines. Instead, Bim was upregulated in immature T cell lines tested. Furthermore, treatment of Jurkat cells with Tat and Taxol showed not only the cleavage of BimEL, but also its hyperphosphorylation, implicating the existence of diverse regulations of Bim under different conditions, such as cell types, apoptotic signals, maybe even different developmental stages of cells. The unique modification pattern of BimEL in Tat and Taxol-treated cells further supports the notion that Tat and Taxol may share a similar mechanism in inducing apoptosis. A paper based on this study is under its way.

In summary, our working model of Tat-induce apoptosis is the following: Tat targets microtubules and perturbs microtubule dynamics, which may activate a kinase(s) to hyperphosphorylate BimEL. This hyperphosphorylated BimEL may be more apoptotic and tip the balance between the pro-apoptotic activities and anti-apoptotic activities in cells and trigger the activation of the downstream caspase cascade. The activated caspases will further cleave and activate the full-length BimEL and push the progression of apoptosis forward.

Note: I have finished this project and graduated from UC Berkeley on Dec. 18, 2003. This is the final annual summary report to terminate the grant. Attached please find two publications resulting from this project under the support of the fellowship.

The EMBO Journal Vol. 21 No. 24 pp. 6801–6810, 2002

HIV-1 Tat targets microtubules to induce apoptosis, a process promoted by the pro-apoptotic Bcl-2 relative Bim

Dan Chen, Michael Wang[1], Sharleen Zhou and Qiang Zhou[2]

Department of Molecular and Cell Biology, University of California at Berkeley, Berkeley, CA 94720-3206 and [1]Department of Pediatrics, University of Colorado Health Sciences Center and Division of Basic Immunology, National Jewish Medical and Research Center, Denver, CO, USA

[2]Corresponding author
e-mail: qzhou@uclink4.berkeley.edu

Depletion of CD4+ T cells is the hallmark of HIV infection and AIDS progression. In addition to the direct killing of the viral-infected cells, HIV infection also leads to increased apoptosis of predominantly uninfected bystander cells. This is mediated in part through the HIV-1 Tat protein, which is secreted by the infected cells and taken up by uninfected cells. Using an affinity-purification approach, a specific and direct interaction of Tat with tubulin and polymerized microtubules has been detected. This interaction does not affect the secretion and uptake of Tat, but is critical for Tat to induce apoptosis. Tat binds tubulin/microtubules through a four-amino-acid subdomain of its conserved core region, leading to the alteration of microtubule dynamics and activation of a mitochondria-dependent apoptotic pathway. Bim, a pro-apoptotic Bcl-2 relative and a transducer of death signals initiated by perturbation of microtubule dynamics, facilitates the Tat-induced apoptosis. Our findings reveal a strategy by which Tat induces apoptosis by targeting the microtubule network. Thus HIV-1 Tat joins a growing list of pathogen-derived proteins that target the cytoskeleton of host cells.
Keywords: apoptosis/Bim/HIV-1/microtubule/Tat

Introduction

Human immunodeficiency virus type 1 (HIV-1) is the etiological agent for the acquired immunodeficiency syndrome (AIDS). HIV-1 encodes a small *trans*-acting regulatory protein, Tat, which is absolutely essential for viral replication and is conserved in the genomes of all primate lentiviruses (Jones and Peterlin, 1994). A primary role of Tat is in regulating productive and processive transcription from the HIV-1 long terminal repeat (LTR). The past decade has been a watershed for the biochemical analysis of the mechanism of Tat stimulation of HIV-1 transcription. In addition to this HIV-1-specific activity, Tat has also been shown to impinge upon many cellular functions, some of which are consistent with the fact that Tat can be secreted by the HIV-infected cells and act upon the neighboring bystander cells (Frankel and Pabo, 1988; Ensoli *et al.*, 1990; Ensoli *et al.*, 1993). Although the mechanisms for the secretion and uptake of Tat are mostly unclear, it is these unique properties that enable Tat to regulate cytokine gene expression and immune cell hyperactivation (Ott *et al.*, 1997), stimulate the growth of Kaposi's sarcoma cells (Ensoli *et al.*, 1990) and induce apoptosis of uninfected T cells (Li *et al.*, 1995; Westendorp *et al.*, 1995; Bartz and Emerman, 1999). Apoptosis contributes to the massive depletion of CD4+ T cells and consequently to the loss of immune competence during HIV-1 infection (Meyaard *et al.*, 1992; Fauci, 1993). Although the mechanisms controlling apoptosis are likely to be multifactorial, Tat and a few other HIV-1 gene products appear to contribute in part to the increased apoptosis associated with AIDS (Roshal *et al.*, 2001).

The mechanisms by which Tat affects the diverse cellular functions are largely unknown. Here, we used an epitope-tagging and affinity-purification approach to identify Tat-associated cellular factors that may regulate or mediate the diverse activities of Tat. This has led to the identification of a specific and direct interaction between Tat and the αβ-tubulin dimer and polymerized microtubules in the cytoplasm of the cell. The Tat–tubulin interaction does not contribute to the secretion and uptake of Tat but appears to be critical for Tat to induce apoptosis in Jurkat T cells. Tat binds tubulin/microtubules through a four-amino-acid subdomain of its evolutionarily conserved core region, and this interaction alters microtubule dynamics, leading to the activation of a mitochondria-dependent apoptotic pathway.

The Bcl-2 family plays a key role in apoptosis by regulating the release of cytochrome c from the mitochondria (Budihardjo *et al.*, 1999). Bim, a pro-apoptotic Bcl-2 family member with only the BH3 domain, induces apoptosis by antagonizing the activity of the anti-apoptotic Bcl-2 family members (O'Connor *et al.*, 1998). In lymphocytes, Bim has been shown to be a dominant transducer of certain apoptotic signals including microtubule perturbation (Bouillet *et al.*, 1999) and activated T-cell death (Hildeman *et al.*, 2002). Here, we showed that Bim facilitates the Tat-induced apoptosis, as over-expression of Bim_L, one of the differentially spliced isoforms of Bim, sensitizes Tat-induced apoptosis. Furthermore, the Bim-deficient lymphocytes are more resistant than the wild-type cells to the killing effect of Tat. Together, our findings reveal a novel strategy by which Tat promotes the killing of the host cells by targeting the microtubule network in a process facilitated by Bim.

Results

Direct and specific interaction of the HIV-1 Tat protein with the αβ-tubulin dimer and polymerized microtubules in the cytoplasm

To identify Tat-associated cellular factors that may regulate or mediate the diverse activities of Tat (Jeang

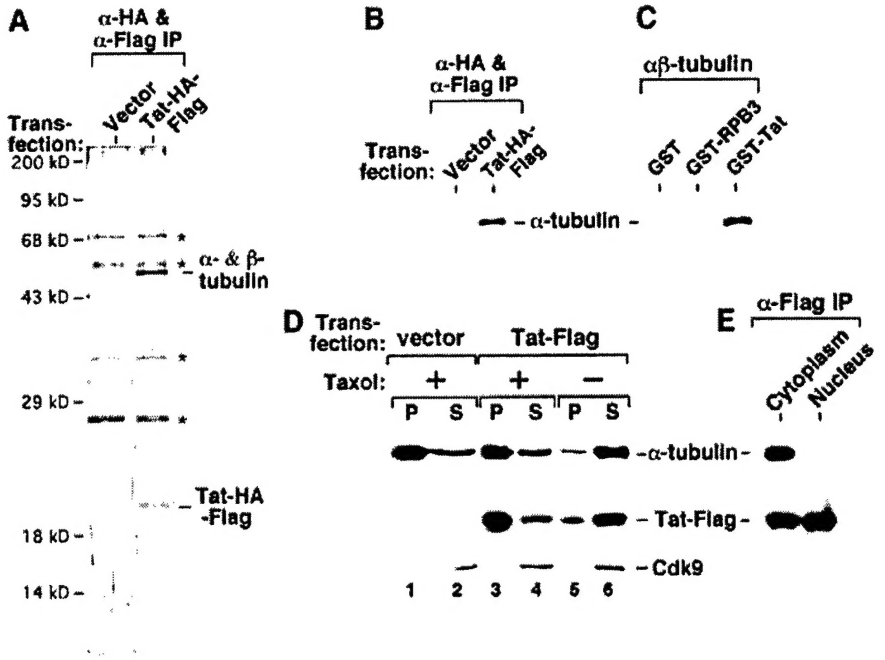

Fig. 1. A direct and specific interaction of Tat with the αβ-tubulin dimer and polymerized microtubules in the cytoplasm. **(A)** Affinity-purified Tat–HA–Flag associates with the αβ-tubulin dimer. Whole-cell lysates from 293T cells transfected with either an empty vector or a vector expressing Tat–HA–Flag were subjected to two rounds of immunoprecipitation with anti-Flag and anti-HA affinity-beads. Upon final elution with the HA peptide, Tat–HA–Flag and its associated factors (α-HA & α-Flag IP) were analyzed by SDS–PAGE and silver staining. Non-specific bands are denoted by asterisks. A specific 50 kDa Tat-associated band was recovered from the gel and digested with trypsin. Microsequencing analysis of the tryptic peptides identified it as a mixture of α- and β-tubulin. **(B)** The association of the tubulin dimer with the affinity-purified Tat–HA–Flag was confirmed by western blotting with antibodies specific for α-tubulin. **(C)** A GST pull-down assay reveals a direct interaction between immobilized GST–Tat and purified αβ-tubulin dimer. GST–RBP3 and GST alone were used as controls. Tubulin dimers associated with the beads were analyzed by anti-α-tubulin western blotting. **(D)** Tat also interacts with the polymerized microtubules. Cleared lysate of 293T cells transfected with either an empty vector or a Tat–Flag-expressing construct was incubated with (+) or without (–) taxol and then subjected to ultracentrifugation as described (Puthalakath *et al.*, 1999). The levels of microtubule/tubulin, Tat–Flag and transcription factor Cdk9 in the pellet (P) and supernatant (S) were determined by western blotting. Cdk9 served as an internal control and remained in the supernatant under both (+) and (–) taxol conditions as expected. **(E)** The Tat–tubulin interaction occurs in the cytoplasm. Cytoplasmic and nuclear extracts were prepared from 293T cells transfected with a Tat–Flag-expression construct and subjected to anti-Flag immunoprecipitation. The precipitates were analyzed for the presence of α-tubulin and Tat–Flag by western blotting.

et al., 1999), a construct expressing HA and Flag double-tagged Tat (Tat–HA–Flag) was transiently transfected into human 293T cells. Tat and its associated proteins were isolated from the cell lysate by two rounds of affinity purification (O'Keeffe *et al.*, 2000) and visualized by silver staining. A 50 kDa protein associated specifically with Tat–HA–Flag (Figure 1A). Microsequencing analysis identified it as a mixture of α- and β-tubulins, which are similar in molecular weight, known to form heterodimers and function as the building blocks of microtubules. The association of the tubulin dimer with Tat–HA–Flag was confirmed by western blotting with specific anti-α-tubulin antibodies (Figure 1B). In control experiments, anti-Flag immunoprecipitates from cells expressing several unrelated Flag-tagged proteins did not show any bound tubulin (data not shown), revealing the specificity of the Tat–tubulin interaction. A direct interaction between Tat and purified αβ-tubulin dimer (Sigma) was further demonstrated in a pull-down assay using immobilized GST–Tat (Figure 1C).

To determine whether Tat also binds to polymerized microtubules, cleared lysate from Tat–Flag-transfected 293T cells was treated with the microtubule-stabilizing drug taxol. Microtubules and microtubule-associated proteins were then separated from the soluble fraction by ultracentrifugation (Puthalakath *et al.*, 1999). While ~85% of Tat remained with free tubulin in the supernatant of an untreated lysate, about the same percentage of Tat was precipitated with the polymerized microtubules in the taxol-treated lysate (Figure 1D), indicating an interaction of Tat with the assembled microtubules.

Tat is best known for its nuclear transcriptional activity, whereas tubulin and microtubules reside in the cytoplasm in non-mitotic cells. To determine the location of the Tat–tubulin interaction, cytoplasmic and nuclear extracts were prepared from 293T cells transfected with a Tat–Flag-expression construct (Dignam *et al.*, 1983). Tat was detected in the anti-Flag immunoprecipitates derived from both extracts. However, only the cytoplasmic Tat interacted with the tubulin dimer (Figure 1E), suggesting the cytoplasm as a likely location for this interaction.

Tat binds tubulin through a four-amino-acid segment within its conserved core region

To map the tubulin-binding domain in Tat, a panel of GST–Tat fusion proteins containing various N- and C-terminally truncated Tat were adjusted to the same concentration and examined for their abilities to interact

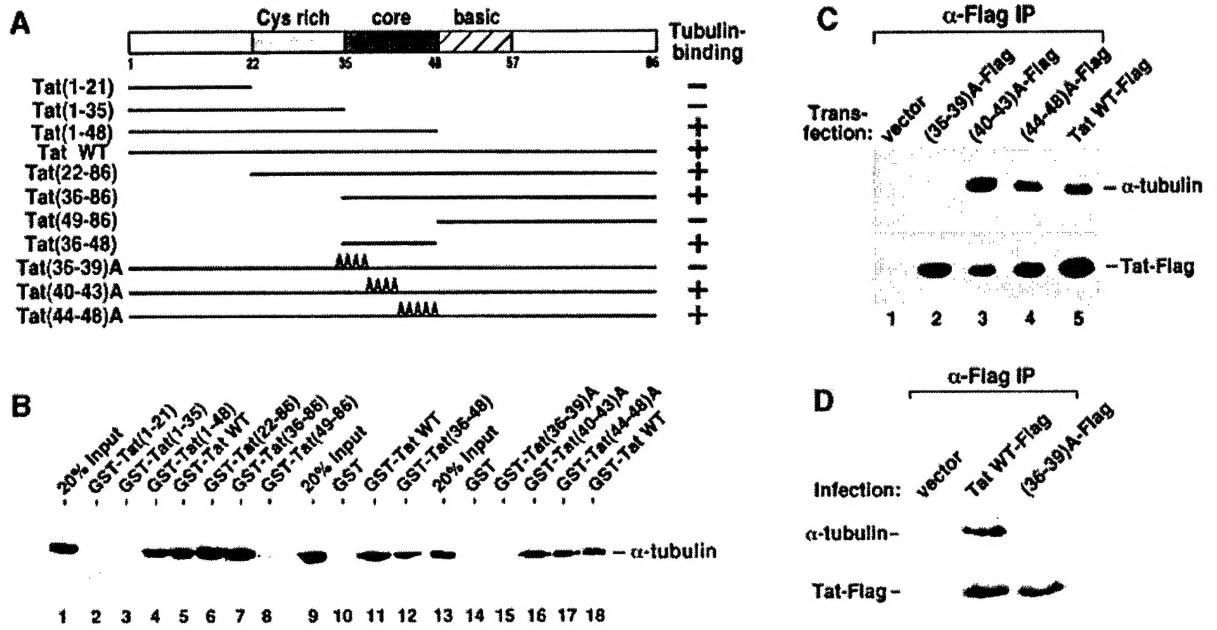

Fig. 2. Tat binds tubulin through a four-amino-acid subdomain within its conserved core region. (**A**) Domain structures of wild-type Tat, N- or C-terminally truncated Tat and alanine (A) substitution Tat mutants. The abilities of these Tat proteins to bind to αβ-tubulin dimers *in vitro* are summarized in the column on the right. The core region (amino acids 36–48) highly conserved among the various lentiviral Tat proteins is indicated as a dark-shaded box in the middle of Tat. (**B**) A GST pull-down assay identifies a four-amino-acid tubulin-binding subdomain in Tat. A panel of immobilized GST–Tat fusion proteins containing wild-type and various Tat mutants were adjusted to the same level (1 μg) and examined for their interactions with the purified αβ-tubulin dimer (1 μg) under conditions described previously (Chen *et al.*, 1999). After extensive washes, the Tat-associated tubulin was detected by western blotting. (**C**) The four-amino-acid subdomain of Tat is also critical for the Tat–tubulin binding *in vivo*. Whole-cell lysates from 293T cells transfected with the indicated Tat constructs were subjected to anti-Flag immunoprecipitation and the precipitates were analyzed by western blotting for the presence of α-tubulin and the various Tat–Flag proteins. (**D**) The Tat–tubulin interaction occurs in retroviral-infected Jurkat T cells. Driven by the MuLV LTR, WT Tat–Flag and Tat(36–39)A-Flag were expressed from the pBabe-puro retroviral vector under infection conditions. The empty vector (pBabe-puro) provided a negative control. Cleared lysates from the infected cells were subjected to anti-Flag immunoprecipitation and the precipitates were analyzed for the presence of Tat–Flag and its associated tubulin by western blotting.

with the purified αβ-tubulin dimer (Figure 2A and B). A 13-amino-acid 'core' region (amino acids 36–48 of HIV-1 Tat) which is highly conserved among the various Tat proteins encoded by the lentiviruses HIV-1, HIV-2, SIV and EIAV (Jones and Peterlin, 1994) was found to be both necessary and sufficient for the Tat–tubulin interaction (Figure 2B, lanes 1–12). While substitutions of amino acids 40–43 or 44–48 with alanines in the Tat core region had virtually no effect on the Tat–tubulin interaction, substitutions of the first four residues (36–39) in a mutant GST–Tat termed (36–39)A significantly impaired this interaction (lanes 13–18). These four residues (Val–Cys–Phe–Ile) appeared to be collectively required for the Tat–tubulin interaction, since individual alanine substitutions of the four residues showed no significant impact (data not shown). The same four-amino-acid subdomain of Tat is also critical for the Tat–tubulin binding in 293T cells, as evidenced by the lack of any detectable interaction between the transfected Tat(36–39)A–Flag and the endogenous tubulin despite the stable expression of the Tat mutant (Figure 2C).

The dependence on the four-amino-acid subdomain for the Tat–tubulin interaction was also examined in infected Jurkat T cells where Tat was produced from a retroviral vector to mimic the HIV infection conditions. Flag-tagged wild-type Tat and (36–39)A were cloned into the pBabe-puro vector (Morgenstern and Land, 1990) under the control of the MuLV LTR. The retroviral constructs were transfected into Phoenix retrovirus packaging cells and the viral supernatants used to infect Jurkat T cells. Again, wild-type Tat but not (36–39)A produced by the viruses associated with tubulin in anti-Flag immunoprecipitates (Figure 2D), revealing the dependence of Tat on the same four-amino-acid subdomain for binding tubulin in infected Jurkat cells. Furthermore, by using a retroviral infection system which produces Tat at close to physiological level, this result also ruled out Tat over-expression as a cause for the observed Tat–tubulin interaction in transfected 293T cells.

Mutation of the tubulin-binding domain in Tat does not affect the release and cytoplasmic uptake of Tat

In acutely HIV-infected cells or cells transfected with a Tat-expressing construct, efficient expression of Tat results in its release into the medium in the absence of any cell lysis (Ensoli *et al.*, 1990, 1993), and the secreted protein can then be taken up by bystander cells (Ensoli *et al.*, 1993; Frankel and Pabo, 1988). Although the mechanisms remain to be elucidated, these properties have enabled Tat to exert a number of biological effects on bystander cells (Jeang *et al.*, 1999). Because the microtubule network is intimately involved in intracellular protein trafficking and transport, an assay described

previously (Ensoli *et al.*, 1993) that measures the coupled release and uptake of Tat was used to examine the role of the Tat–tubulin interaction in this process. Human 293T cells transfected with constructs expressing Flag-tagged wild-type Tat, Tat(36–39)A, Cdk9 or cyclin T1 were mixed 1:1 with untransfected cells at 24 h post-transfection. The co-cultivated cells were analyzed 1 day later by anti-Flag immunofluorescence staining (Figure 3A). Using Hoechst 3342-generated nuclear DNA staining patterns as a reference, human transcription factors Cdk9 and cyclin T1 were expressed as nuclear proteins in ~20% of transfected cells and neither protein was released into the medium and taken up by untransfected cells. In contrast, wild-type Tat was found predominantly in the cytoplasmic region of every cell within the entire population (Figure 3A), indicating a coupled release and cytoplasmic uptake of Tat by the co-cultivated cells. These data agree with the previous observations that bystander cells take up the secreted Tat in mostly the cytoplasm and only a small portion can reach the nucleus to activate HIV-1 transcription (Ensoli *et al.*, 1993). Strong whole-cell staining of Tat was also observed in a small number of cells (data not shown), which were probably the transfected Tat-producing cells. Importantly, both wild-type Tat and Tat(36–39)A defective in tubulin binding demonstrated a similar efficiency in their coupled release and cytoplasmic uptake (Figure 3A), which was observed over a broad range of Tat concentrations (data not shown). Thus the Tat–tubulin interaction did not appear to contribute to the coupled release and uptake of Tat.

The tubulin-binding domain in Tat is required for Tat-induced apoptosis but not for G_1 delay

Extracellular Tat has been shown to induce apoptosis and increase sensitivity to apoptotic signals in both primary $CD4^+$ T cells and T-cell lines, contributing in part to the progressive loss of T cells associated with AIDS (Li *et al.*, 1995; Westendorp *et al.*, 1995; Bartz and Emerman, 1999). Since the Tat–tubulin interaction is not required for the release and uptake of Tat, we investigated whether it is required for Tat-induced apoptosis. Recombinant Tat proteins were added to the cultures of Jurkat T cells and their apoptotic effects were analyzed by flow cytometry. Treatment of cells with wild-type Tat, an alanine-substitution mutant Tat(44–48)A or a transcriptionally inactive Tat mutant C22G, all three of which displayed a similar and strong tubulin-binding capability (Figure 2 and data not shown), caused significant and dose-dependent apoptosis as indicated by increases in the amount of hypodiploid nuclei (Figure 3B). In contrast, Tat(36–39)A was completely incapable of inducing apoptosis, suggesting that the tubulin binding but not the transcriptional activity of Tat is critical for Tat-induced apoptosis.

In support of the above data obtained in Jurkat cells with recombinant Tat proteins, sustained expression from stably transfected constructs of wild-type Tat and three transcriptionally inactive Tat mutants, C22G, H33A and K41A (Rice and Carlotti, 1990), which are active in tubulin binding (data not shown) suppressed colony formation of 293T cells more potently than did expression of Tat(36–39)A (Figure 3C). This result further underscores the importance of the tubulin-binding activity of Tat in induction of apoptosis.

The caspase family of cysteine proteases plays a pivotal role in mediating apoptosis through proteolysis of specific targets. In Jurkat cells treated with wild-type Tat, a cleaved 85 kDa fragment of PARP, a target of the downstream effector caspases such as caspase-3 and caspase-6 (Lazebnik *et al.*, 1994), was observed (Figure 3D), indicating an activation of the caspase cascade. Although Tat(36–39)A failed in this regard, it is still active in preventing the phosphorylation of retinoblastoma protein pRb (Figure 3E), an activity thought to be responsible for the Tat-induced G_1 delay (Kundu *et al.*, 1998).

Because the tubulin-binding subdomain of Tat (amino acids 36–39) contains Phe38, a residue essential for Tat to transactivate the HIV-1 LTR (Rice and Carlotti, 1990), it is not feasible to examine the apoptotic activity of the mutant HIV-1 virus expressing Tat(36–39)A, which would express few if any HIV-1 proteins. To circumvent this limitation and analyze the apoptotic effect of Tat expressed at close to physiological level, we expressed wild-type Tat and Tat(36–39)A from recombinant retroviruses in Jurkat T cells under the infection conditions. Infected cells co-expressing GFP and Tat from two open reading frames separated by an IRES in the pMX-Tat-IRES-GFP retroviral vector (Liu *et al.*, 1997) were analyzed by flow cytometry to detect apoptotic cells which were able to absorb propidium iodide. After subtracting the background level of apoptosis caused by the control virus expressing only GFP, the virus-produced wild-type Tat induced 7.6 times more apoptosis than did (36–39)A, revealing a key role of the tubulin-binding domain in this process (Figure 3F).

Tat induces apoptosis by preventing microtubule depolymerization

Microtubule dynamics, a fundamental property of microtubules, is critical for diverse cellular functions and regulated by many factors. Persistent perturbation of microtubule dynamics by microtubule-damaging drugs is known to cause apoptosis (Sorger *et al.*, 1997; Wang *et al.*, 2000). With the observation that the Tat–tubulin interaction may contribute to apoptosis, we investigated whether Tat may exert this effect by altering microtubule dynamics. Extracts containing free tubulin dimers (S), or polymerized microtubules (P) or a mixture of both (T) were each prepared from Jurkat cells treated with wild-type Tat, Tat(36–39)A or the microtubule-perturbation drugs taxol or nocodazole and were then analyzed by anti-α-tubulin western blotting (Figure 4A). As expected, the microtubule-stabilizing drug taxol and the destabilizing drug nocodazole altered the partitioning of microtubules and tubulin in opposite directions and both caused significant apoptosis (Figure 4A). Like taxol, wild-type Tat, but not Tat(36–39)A, also caused a significant stabilization of microtubules and a concurrent reduction of the level of unpolymerized tubulin in the cell. The broad-spectrum caspase inhibitor zVAD-fmk inhibited the Tat-induced apoptosis, but had no effect on Tat stabilization of microtubules, indicating that this latter event occurred during the initiation of apoptosis and was not simply a consequence of caspase activation.

Immunofluorescence studies further supported the idea that Tat acts to prevent microtubule depolymerization (Figure 4B). In untreated cells, microtubule fibers appeared

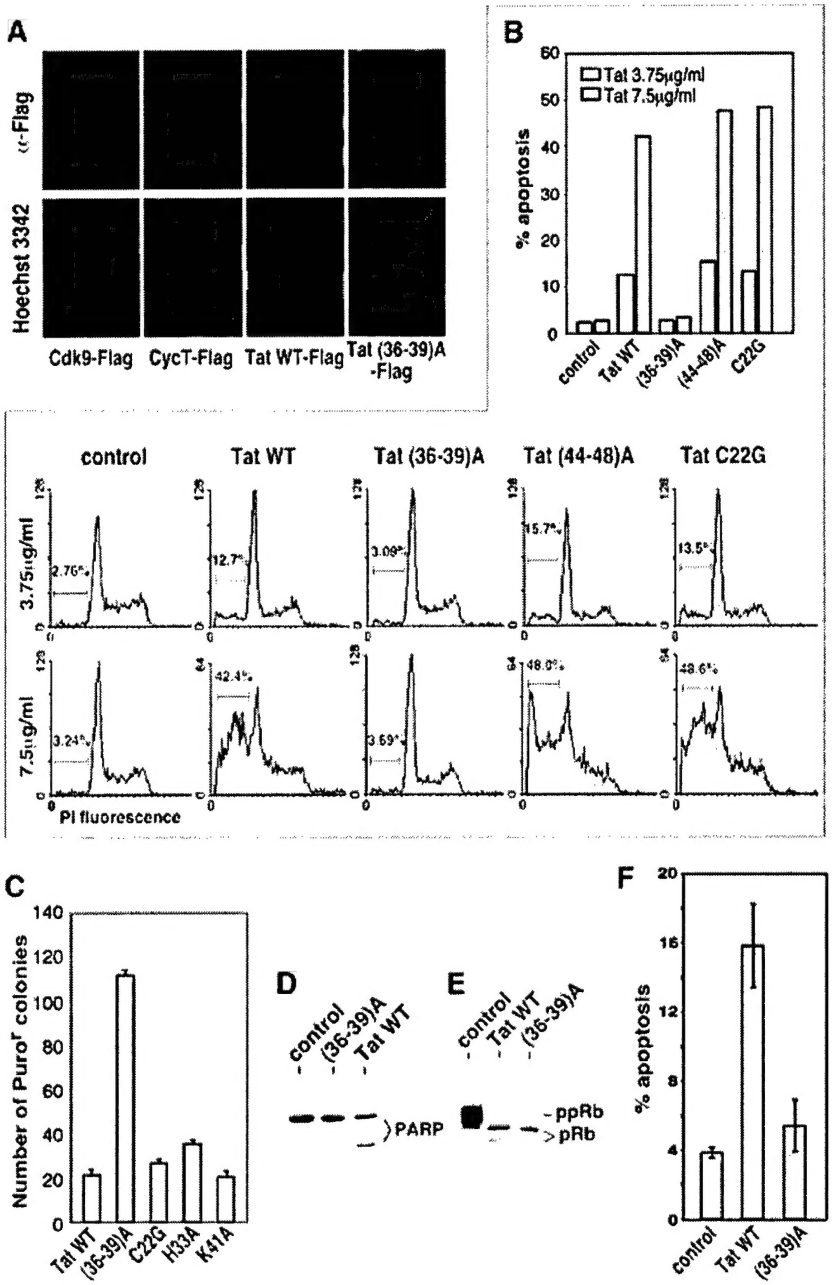

Fig. 3. The tubulin-binding domain of Tat is required for Tat-induced apoptosis but not for G_1 delay. (**A**) Mutation of the tubulin-binding domain in Tat does not affect the release and cytoplasmic uptake of Tat. Transfected 293T cells expressing Flag-tagged wild-type Tat, Tat(36–39)A, Cdk9 or cyclin T1 were mixed 1:1 with untransfected cells at 24 h post-transfection. The co-cultivated cells were analyzed 1 day later by anti-Flag immunofluorescence staining. The Hoechst 3342-generated nuclear DNA staining pattern was used as a reference. (**B**) The tubulin-binding activity of Tat is required for Tat-induced apoptosis. Recombinant wild-type Tat and the indicated Tat mutants were added at two different concentrations into the cultures of Jurkat cells and the percentage of apoptotic cells with hypodiploid nuclei was analyzed by flow cytometry and summarized in a column chart. (**C**) Sustained expression of Tat active in tubulin-binding suppresses colony formation of 293T cells. Constructs expressing the indicated Tat proteins were co-transfected with pBabe-Puro conferring puromycin resistance at a 30:1 ratio into 293T cells. The expression levels of the transfected Tat proteins were similar (data not shown). The number of puromycin-resistant colonies was counted after 2 weeks of incubation and plotted. (**D**) Tat treatment of Jurkat cells causes the cleavage of PARP. Recombinant wild-type Tat and mutant Tat(36–39)A were added at 3.75 μg/ml into the cultures of Jurkat cells. Whole-cell lysates were prepared 18 h later and analyzed by anti-PARP western blotting. (**E**) Tat prevents phosphorylation of the retinoblastoma protein (pRb) independent of its tubulin-binding activity. Whole-cell lysates from Jurkat cells treated with either wild-type Tat or Tat(36–39)A were analyzed for the presence of the phosphorylated (ppRb) and under-phosphorylated (pRb) retinoblastoma proteins by western blotting as described (Kundu *et al.*, 1998). (**F**) Expression of wild-type Tat but not Tat(36–39)A under retroviral infection conditions causes apoptosis. Wild-type Tat or Tat(36–39)A was co-produced with GFP from an IRES-containing retroviral vector. The infected GFP-positive Jurkat cells were gated by flow cytometry and the percentage of cell death determined by propidium iodide uptake. A similar level of expression of the wild-type and mutant Tat was detected in the infected cells (data not shown). Viruses that expressed GFP alone were used as a control.

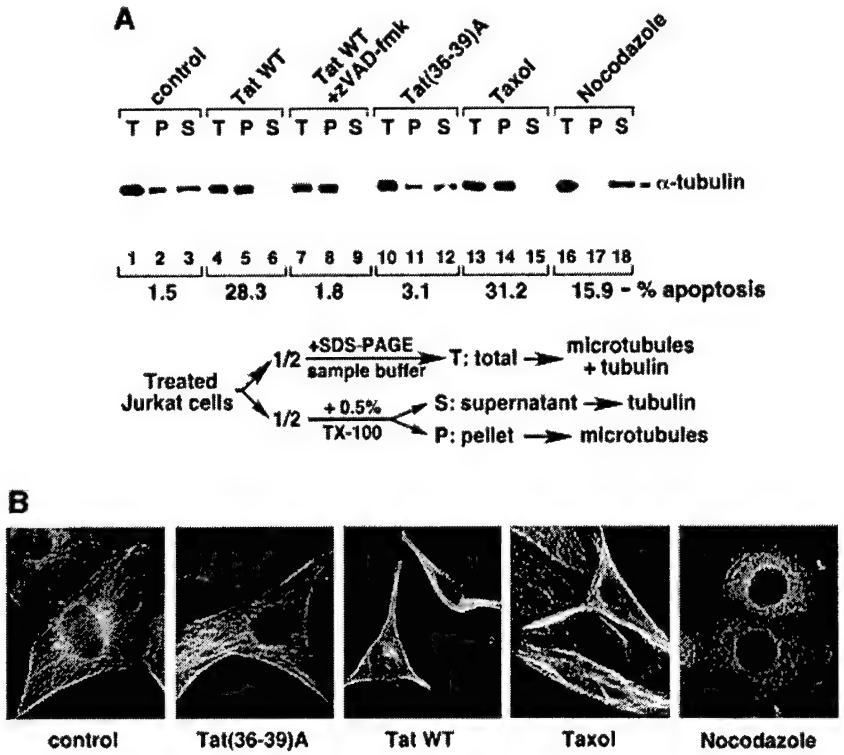

Fig. 4. Tat induces apoptosis by preventing microtubule depolymerization. (**A**) Tat treatment of Jurkat cells stabilizes microtubules and this effect precedes the activation of caspases. Upon treatment of Jurkat cells with the indicated agents, half the cells were boiled in SDS–PAGE sample buffer to obtain a mixture of total tubulin and microtubules in the cell (T). The other half were extracted with a buffer containing 0.5% Triton X-100 and subjected to centrifugation to obtain the pellet (P) containing assembled microtubules and supernatant (S) containing free tubulin dimers as described (Nguyen *et al.*, 1999). The amount of tubulin/microtubules present in each fraction was analyzed by anti-α-tubulin western blotting. In a parallel experiment, apoptosis induced by the various agents was determined by flow cytometry as in Figure 3A, and the percentage of apoptosis was indicated below the western blot. (**B**) Alterations of the cellular microtubule network upon Tat treatment. NIH 3T3 cells were treated with the indicated reagents and analyzed by immunofluorescence staining using α-tubulin antibodies to visualize the microtubule network.

to fill the whole cytoplasm and extend virtually the entire distance to the edges of the cell. While microtubules were significantly fragmented in cells exposed to nocodazole, microtubule tangling and bundling, particularly in the cell periphery, were observed in taxol-treated cells as reported previously (Liao *et al.*, 1995). Treatment of cells with wild-type Tat, but not with Tat(36–39)A, produced a pattern of microtubule network similar to that of taxol-treated cells. These observations, together with the above biochemical data, suggest that the Tat–tubulin interaction prevents microtubule depolymerization, which may initiate a signaling pathway leading to apoptosis.

Tat induces apoptosis through the mitochondria pathway

The taxol-perturbation of microtubules is known to induce apoptosis through a mitochondria-dependent pathway (André *et al.*, 2000; Wang *et al.*, 2000). One characteristic of this pathway is the cleavage and activation of caspase-9 (Budihardjo *et al.*, 1999). Like taxol, treatment of Jurkat cells with wild-type Tat, but not with Tat(36–39)A, also caused efficient cleavage of caspase-9 (Figure 5A), suggesting that the death signals initiated by Tat perturbation of microtubules also transmit through the mitochondria pathway. In support of this model, Tat has previously been shown to cause changes in mitochondrial membrane permeability (Macho *et al.*, 1999; Ferri *et al.*, 2000).

Previous reports have also suggested that Tat may induce apoptosis by upregulating the expression of FasL (Westendorp *et al.*, 1995) and caspase-8 (Bartz and Emerman, 1999), both of which presumably signal through the death-receptor pathway. To investigate the contribution of this pathway to Tat-induced apoptosis, the apoptotic activity of Tat was examined in mouse A20 cells stably expressing a dominant negative form of the Fas adaptor molecule FADD, which has been shown to block the death-receptor pathway completely (Zhang and Winoto, 1996; Newton *et al.*, 1998). As expected, the dominant negative FADD efficiently inhibited apoptosis induced by the anti-Fas antibody but had no effect on the taxol-induced apoptosis (Figure 5B). Like taxol, Tat caused a similar level of apoptosis in both cells, suggesting that the Tat-induced apoptosis was unaffected by inhibition of the death-receptor pathway.

Bim promotes Tat-induced apoptosis

The pro-apoptotic Bcl-2 relative Bim induces apoptosis by antagonizing the activity of the anti-apoptotic Bcl-2 family members (O'Connor *et al.*, 1998). In lymphocytes, Bim has been shown to be a major transducer of certain apoptotic signals including microtubule perturbation

(Bouillet *et al.*, 1999). Since both Tat and taxol may induce apoptosis by perturbing microtubule dynamics, the role of Bim_L, one of the differentially spliced isoforms of Bim, in Tat- and taxol-induced apoptosis was investigated (Figure 5C). Cells co-expressing Bim_L and Bcl-2 were significantly more sensitive to taxol- and Tat-induced apoptosis than cells expressing Bcl-2 alone. In contrast, a similar level of apoptosis was induced in both cell types by TNFα, which transduces apoptotic signals through the death-receptor pathway. This sensitizing effect of Bim_L on Tat- and taxol-induced apoptosis further underscores the importance of Bim_L in mediating apoptosis induced by agents that impinge upon microtubules.

It has been shown that Bim-deficient lymphocytes are more resistant than wild-type cells to certain apoptotic stimuli such as cytokine deprivation, calcium ion flux and taxol-induced microtubule perturbation (Bouillet *et al.*, 1999) and activated T-cell death (Hildeman *et al.*, 2002). Since Tat may induce apoptosis by altering microtubule dynamics, the sensitivity of T cells derived from $Bim^{-/-}$ knockout mice to Tat-induced apoptosis was compared with that of wild-type cells (Figure 5D). Bim-deficient T cells have been shown to display a somewhat decreased basal level of apoptosis after overnight culturing (Bouillet *et al.*, 1999; Hildeman *et al.*, 2002; data not shown). After subtracting the respective basal levels to reveal specifically the Tat-induced apoptosis, the $Bim^{-/-}$ cells displayed an increased resistance to Tat compared with the wild-type cells, highlighting a critical role of Bim in Tat-induced apoptosis. It has been shown that the death-receptor-induced apoptosis and apoptosis signaling pathways regulated by members of the Bcl-2 family are distinct in their dependence on the Bim protein (Strasser *et al.*, 1995; Bouillet *et al.*, 1999). The stimulating effect of Bim on Tat-induced apoptosis further suggests that Tat induces apoptosis predominantly through the mitochondria-dependent pathway and not the death-receptor pathway.

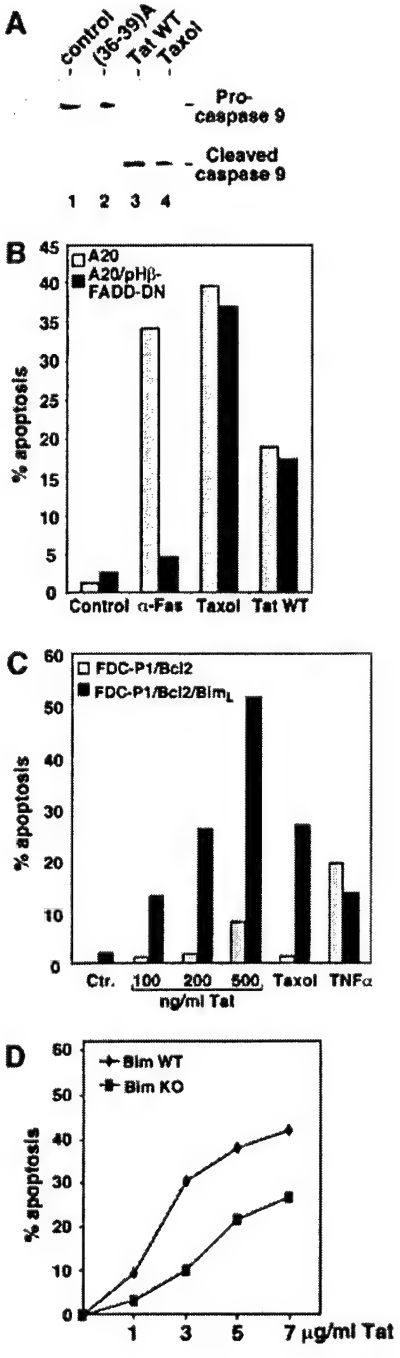

Fig. 5. Tat induces apoptosis through the mitochondria pathway. (**A**) Tat treatment of Jurkat cells causes efficient cleavage of pro-caspase-9. Anti-caspase 9 western blotting was performed to detect procaspase-9 and cleaved caspase-9 in whole-cell lysates of Jurkat cells treated with the indicated agents. (**B**) Inhibition of the death-receptor pathway by dominant negative FADD does not prevent Tat-induced apoptosis. Mouse A20 cells as well as an A20 derivative which stably expresses dominant negative FADD were treated with the indicated apoptosis-inducing agents. The percentage of apoptosis was determined by flow cytometry, and the data shown were representative of four independent experiments. (**C**) Bim_L sensitizes Tat-induced apoptosis. Mouse FDC-P1 cells which stably express Bcl-2 or Bcl-2 plus Bim_L were treated with the indicated apoptosis-inducing agents. The percentage of apoptosis was determined by flow cytometry, and the data shown were representative of three independent experiments. (**D**) Bim-deficient T lymphocytes are more resistant than wild-type cells to Tat-induced apoptosis. T cells were purified from spleens and lymph nodes of wild type and $Bim^{-/-}$ knockout mice and treated with different amounts of Tat as indicated in the figure. The T cells were stained with propidium iodide after 12 h of culture, and cell death was determined by flow cytometry.

Discussion

The data presented in this study are consistent with a model that Tat targets microtubules and transduces the death signal through a mitochondria-dependent pathway that is facilitated by the pro-apoptotic Bcl-2 family member Bim. Tat binds to tubulin/microtubules through part of its conserved core region both *in vitro* and under retroviral infection conditions *in vivo*. It will be of interest to determine whether microtubules are also targeted by the conserved regions of HIV-2 Tat and perhaps other lentiviral Tat proteins for apoptosis (Bartz and Emerman, 1999). The amino acid residues of Tat required for the Tat–tubulin interaction differ from those present in the tubulin-binding domains of conventional microtubule-associated proteins (MAPs), which typically contain positively charged residues (Hirokawa, 1994). Although

not directly required for the Tat–tubulin binding (Figure 2), the arginine-rich domain of Tat adjacent to the tubulin-binding subdomain could conceivably provide the positive charge to neutralize the negatively charged tubulin C-termini in order to promote microtubule assembly.

The mechanistic details between Tat stabilization of microtubules and the initiation of the apoptotic-signaling pathway remain to be elucidated. The similarity between Tat and taxol in affecting microtubule dynamics suggests that their apoptotic pathways may share similar mechanisms or themes. Bim_L transduces the death signal initiated by microtubule perturbation, leading to apoptosis through the mitochondria pathway. It is normally sequestered to microtubules and can be released by apoptotic stimuli that impinge upon microtubules. The released Bim_L binds to and neutralizes anti-apoptotic activity of Bcl-2 (Puthalakath *et al.*, 1999). The observation that Bim_L can synergize with Tat and taxol, but not with TNFα, in induction of apoptosis suggests that Bim_L may play a key role in Tat- and taxol-induced apoptosis. In fact, the higher expression level of Bim_L in T lymphocytes than in many other cell types (O'Reilly *et al.*, 2000) may explain the higher sensitivity of the lymphocytes to Tat-induced apoptosis (Li *et al.*, 1995; our unpublished data). A more direct demonstration of a tight link between the cellular level of Bim and the Tat-induced apoptosis is provided by the observation that the Bim-deficient T cells are more resistant than the wild-type cells to the killing effect of Tat. It is worth noting that the $Bim^{-/-}$ cells are not completely resistant to this Tat effect (Figure 5D), suggesting a possibility that other pro-apoptotic members of the Bcl-2 family may work in parallel with Bim to transduce the Tat-induced death signal. Future analyses are necessary to investigate whether Tat may play a direct and specific role in causing the release of Bim_L from microtubules and also to determine the possible involvement of other Bcl-2 family members in mediating Tat-induced apoptosis.

Enhanced apoptosis has been observed in lymph nodes of HIV-1-infected individuals (Fauci, 1993) and in lymphocytes isolated from AIDS patients (Meyaard *et al.*, 1992). Studies using *in situ* labeling of lymph nodes from HIV-infected children and SIV-infected macaques have demonstrated that apoptosis occurs predominantly in bystander cells and not in the productively infected cells themselves (Finkel *et al.*, 1995). Furthermore, *in vitro* co-culture experiments of HIV-1-infected and uninfected cells have indicated that, while uninfected $CD4^+$ cells die by apoptosis, HIV-infected cells are resistant to HIV-induced cell death (Nardelli *et al.*, 1995). These data suggest that the virus may have evolved an ability to induce apoptosis in bystander cells and prevent apoptosis in the infected cells. By targeting the very general microtubule cytoskeleton to induce apoptosis, it is hard to imagine that Tat itself could have accomplished such a high specificity by killing off only the uninfected cells. It is more likely that the death signals initiated by Tat perturbation of microtubule dynamics can be blocked in the HIV-infected cells.

Indeed, HIV has been reported to employ at least two different strategies to prevent the mitochondria-dependent apoptosis in infected cells. Two HIV-encoded proteins can regulate the activities of members of the Bcl-2 family, the main regulators of the mitochondria-dependent apoptotic pathway. HIV-1 Nef activates the phosphatidylinositol-3–PAK complex, which phosphorylates and inactivates the pro-apoptotic Bad protein. Consequently, wild-type Nef, but not a Nef mutant incapable of activating PAK, blocks apoptosis in T cells induced by HIV replication (Wolf *et al.*, 2001). Furthermore, HIV-1 Vpr causes the up-regulation of the levels of the anti-apoptotic Bcl-2, and the down-modulation of the pro-apoptotic Bax (Conti *et al.*, 1998).

In summary, the data presented in this study highlight the ability of Tat to target the microtubule cytoskeleton to induce apoptosis. The cytoskeleton is essential for diverse cellular functions. Many pathogens exploit this versatility and develop different strategies to target the cytoskeleton for a variety of purposes (Finlay and Cossart, 1997). The ability of HIV-1 Tat to induce apoptosis by targeting the microtubule network allows Tat to join a growing list of pathogen-encoded proteins which target the cytoskeleton of host cells.

Materials and methods

Affinity purification of Tat–HA–Flag and its associated proteins

The purification was performed essentially as described (O'Keeffe *et al.*, 2000). 293T cells transiently transfected with a construct expressing Tat–HA–Flag were lysed in a buffer containing 50 mM HEPES–KOH pH 7.8, 500 mM NaCl, 5 mM EDTA, 1% NP-40, 3 mM dithiothreitol and 0.5 mM phenylmethylsulfonyl fluoride. Pre-cleared lysate was then incubated with anti-Flag antibody beads (Sigma) at 4°C for 2 h. After extensive washes in the same buffer, Tat–HA–Flag and its associated proteins were eluted with the Flag peptide. The eluted fraction was subjected to a second round of purification using anti-HA (mAb 12CA5) antibody beads followed by HA peptide elution. Peptide digestion and microsequencing analyses of the Tat-associated proteins were as described (O'Keeffe *et al.*, 2000).

Cell death analyses

Apoptosis was induced in Jurkat T cells by 50 ng/ml TNFα, 10 μM nocodazole, 0.05 μM taxol or the indicated amounts of wild-type and mutant Tat proteins as specified in the figure legends. The broad-spectrum caspase inhibitor zVAD-fmk was used at 20 μM. Cell death was measured by flow cytometric analysis of hypodiploid nuclei stained with 20 μg/ml propidium iodide. For A20-derived cells, 0.5 μM taxol, 20 ng/ml Fas antibody or 15 μg/ml Tat were used to induce apoptosis. For colony formation assay, the Tat-expressing constructs were co-transfected with pBabe-Puro conferring puromycin resistance at a 30:1 ratio into 293T cells. The transfected cells were diluted 2 days later into fresh Dulbecco's modified Eagle's medium (DMEM) plus 10% fetal bovine serum (FBS) and 0.5 μg/ml of puromycin. The number of drug-resistant colonies was counted 2 weeks later.

Coupled release/uptake of Tat and immunofluorescence analysis

The procedure was essentially as described (Ensoli *et al.*, 1993) with some modifications. 293T cells transfected with constructs expressing Tat–Flag or control proteins were mixed 1:1 with untransfected cells 24 h post-transfection. The localization of the transfected proteins in the co-cultivated cells was determined 1 day later by immunofluorescence staining. Cells were fixed in methanol at –20°C for 10 min, blocked with 10% BSA/0.1% Tween-20 in PBS and incubated with anti-Flag mouse monoclonal antibody (2 μg/ml; Sigma) followed by Texas Red-conjugated donkey anti-mouse IgG (7 μg/ml; Jackson ImmunoResearch).

Association of Tat with assembled microtubules

The procedure was essentially as described (Puthalakath *et al.*, 1999) with some modifications. Tat–Flag-transfected 293T cells were lysed in a buffer containing 20 mM Tris–HCl pH 7.4, 135 mM NaCl, 1.5 mM $MgCl_2$, 1% Triton X-100, 10% glycerol, 2 mM dithiothreitol and 0.5 mM phenylmethylsulfonyl fluoride. Lysate was centrifuged at 10 000 r.p.m. for 10 min to remove debris. The cleared lysate was treated with 5 μg/ml

of taxol at 37°C for 20 min to reassemble microtubules and the reaction mixture was loaded on top of a 20% sucrose cushion. Microtubules and their associated proteins were isolated by ultracentrifugation at 100 000 *g* for 1 h.

Mice

Female 15-week-old Bim wild-type mice and Bim-deficient littermate, described previously (Bouillet *et al.*, 1999) and back-crossed 12 times to C57BL/6, were used for all experiments. All mice were kept under specific pathogen-free conditions in the Biological Resource Center at the National Jewish Medical and Research Center.

Bim$^{-/-}$ cell culture

To obtain T cells for cell culture, spleen and lymph nodes (axillary, brachial, inguinal, submandibular, mesenteric and peri-aortic) were homogenized through 100 μm nylon wool strainers. The single-cell suspensions were enriched for T cells by passage through nylon wool (Julius *et al.*, 1973). After nylon wool enrichment, 1×10^6 cells were resuspended in complete tumor medium (s-MEM containing β-mercapto-ethanol, penicillin, streptomycin, glutamine and 10% FBS) with the indicated amount of Tat. T cells were cultured for 12 h and then processed for flow cytometry.

Retroviral infection

pBabe-puro-Tat–Flag or pMX-Tat-IRES-GFP was transfected into Phoenix retrovirus packaging cells by Lipofectmin-Plus reagent (Invitrogen) according to the manufacturer's instructions. Two days later, 70 ml of viral supernatant was mixed with an equal volume of 1×10^6/ml Jurkat cell culture, and polybrene was added to the final concentration of 4 μg/ml. Cells were harvested 2 days post-infection for immunoprecipitation or flow cytometry analyses as indicated in the text and figure legends.

Acknowledgements

We thank the A.Strasser, P.Marrack, R.Tjian, D.Koshland, A.Winoto, R.Heald laboratories, H.Nolla and the University of California at Berkeley cell-sorting facility for technical help and valuable reagents, and K.Luo, J.Mougous and S.Stroschein for comments on the manuscript. This work was supported by grants from the National Institutes of Health (AI-41757) and the American Cancer Society (RSG-01-171-01-MBC) to QZ, and by a US Army Breast Cancer Predoctoral Fellowship to DC (DAMD17-02-1-0321). M.W. is an NICHD Fellow of the Pediatric Scientist Development Program (NICHD K12-HD00850-17).

References

André,N., Braguer,D., Brasseur,G., Gonçalves,A., Lemesle-Meunier,D., Guise,S., Jordan,M.A. and Briand,C. (2000) Paclitaxel induces release of cytochrome c from mitochondria isolated from human neuroblastoma cells. *Cancer Res.*, **60**, 5349–5353.

Bartz,S.R. and Emerman,M. (1999). Human immunodeficiency virus type 1 Tat induces apoptosis and increases sensitivity to apoptotic signals by up-regulating FLICE/caspase-8. *J. Virol.*, **73**, 1956–1963.

Bouillet,P., Metcalf,D., Huang,D.C., Tarlinton,D.M., Kay,T.W., Köntgen,F., Adams,J.M. and Strasser,A. (1999) Proapoptotic Bcl-2 relative Bim required for certain apoptotic responses, leukocyte homeostasis and to preclude autoimmunity. *Science*, **286**, 1735–1738.

Budihardjo,I., Oliver,H., Lutter,M., Luo,X. and Wang,X. (1999) Biochemical pathways of caspase activation during apoptosis. *Annu. Rev. Cell. Dev. Biol.*, **15**, 269–290.

Chen,D., Fong,Y. and Zhou,Q. (1999) Specific interaction of Tat with the human but not rodent P-TEFb complex mediates the species-specific Tat activation of HIV-1 transcription. *Proc. Natl Acad. Sci. USA*, **96**, 2728–2733.

Conti,L. *et al.* (1998) The HIV-1 vpr protein acts as a negative regulator of apoptosis in a human lymphoblastoid T cell line: possible implications for the pathogenesis of AIDS. *J. Exp. Med.*, **187**, 403–413.

Dignam,J.D., Lebovitz,R.M. and Roeder,R.G. (1983) Accurate transcription initiation by RNA polymerase II in a soluble extract from isolated mammalian nuclei. *Nucleic Acids Res.*, **11**, 1475–1489.

Ensoli,B., Barillari,G., Salahuddin,S.Z., Gallo,R.C. and Wong-Staal,F. (1990) Tat protein of HIV-1 stimulates growth of cells derived from Kaposi's sarcoma lesions of AIDS patients. *Nature*, **345**, 84–86.

Ensoli,B., Buonaguro,L., Barillari,G., Fiorelli,V., Gendelman,R., Morgan,R.A., Wingfield,P. and Gallo,R.C. (1993) Release, uptake and effects of extracellular human immunodeficiency virus type 1 Tat protein on cell growth and viral transactivation. *J. Virol.*, **67**, 277–287.

Fauci,A.S. (1993) Multifactorial nature of human immunodeficiency virus disease: implications for therapy. *Science*, **262**, 1011–1018.

Ferri,K.F., Jacotot,E., Blanco,J., Esté,J.A. and Kroemer,G. (2000) Mitochondrial control of cell death induced by HIV-1-encoded proteins. *Ann NY Acad. Sci.*, **926**, 149–164.

Finkel,T.H., Tudor-Williams,G., Banda,N.K., Cotton,M.F., Curiel,T., Monks,C., Baba,T.W., Ruprecht,R.M. and Kupfer,A. (1995) Apoptosis occurs predominantly in bystander cells and not in productively infected cells of HIV- and SIV-infected lymph nodes. *Nature Med.*, **1**, 129–134.

Finlay,B.B. and Cossart,P. (1997) Exploitation of mammalian host cell functions by bacterial pathogens. *Science*, **276**, 718–725.

Frankel,A.D. and Pabo,C.O. (1988) Cellular uptake of the tat protein from human immunodeficiency virus. *Cell*, **55**, 1189–1193.

Hildeman,D.A., Zhu,Y., Mitchell,T.C., Bouillet,P., Strasser,A., Kappler,J. and Marrack,P. (2002) Activated T cell death *in vivo* mediated by pro-apoptotic Bcl-2 family member, Bim. *Immunity*, **16**, 759–767.

Hirokawa,N. (1994) Microtubule organization and dynamics dependent on microtubule-associated proteins. *Curr. Opin. Cell Biol.*, **6**, 74–81.

Jeang,K.T., Xiao,H. and Rich,E.A. (1999) Multifaceted activities of the HIV-1 transactivator of transcription, Tat. *J. Biol. Chem.*, **274**, 28837–28840.

Jones,K.A. and Peterlin,B.M. (1994) Control of RNA initiation and elongation at the HIV-1 promoter. *Annu. Rev. Biochem.*, **63**, 717–743.

Julius,M.H., Simpson,E. and Herzenberg,L.A. (1973) A rapid method for the isolation of functional thymus-derived murine lymphocytes. *Eur. J. Immunol.*, **3**, 645–649.

Kundu,M., Sharma,S., De Luca,A., Giordano,A., Rappaport,J., Khalili,K. and Amini,S. (1998) HIV-1 Tat elongates the G_1 phase and indirectly promotes HIV-1 gene expression in cells of glial origin. *J. Biol. Chem.*, **273**, 8130–8136.

Lazebnik,Y.A., Kaufmann,S.H., Desnoyers,S., Poirier,G.G. and Earnshaw,W.C. (1994) Cleavage of poly(ADP-ribose) polymerase by a proteinase with properties like ICE. *Nature*, **371**, 346–347.

Li,C.J., Friedman,D.J., Wang,C., Metelev,V. and Pardee,A.B. (1995) Induction of apoptosis in uninfected lymphocytes by HIV-1 Tat protein. *Science*, **268**, 429–431.

Liao,G., Nagasaki,T. and Gundersen,G.G. (1995) Low concentrations of nocodazole interfere with fibroblast locomotion without significantly affecting microtubule level: implications for the role of dynamic microtubules in cell locomotion. *J. Cell Sci.*, **108**, 3473–3483.

Liu,X., Sun,Y., Constantinescu,S.N., Karam,E., Weinberg,R.A. and Lodish,H.F. (1997) Transforming growth factor β-induced phosphorylation of Smad3 is required for growth inhibition and transcriptional induction in epithelial cells. *Proc. Natl Acad. Sci. USA*, **94**, 10669–10674.

Macho,A., Calzado,M.A., Jiménez-Reina,L., Ceballos,E., León,J. and Muñoz,E. (1999) Susceptibility of HIV-1-TAT transfected cells to undergo apoptosis. Biochemical mechanisms. *Oncogene*, **18**, 7543–7551.

Meyaard,L., Otto,S.A., Jonker,R.R., Mijnster,M.J., Keet,R.P. and Miedema,F. (1992) Programmed death of T cells in HIV-1 infection. *Science*, **257**, 217–219.

Morgenstern,J.P. and Land,H. (1990) Advanced mammalian gene transfer: high titre retroviral vectors with multiple drug selection markers and a complementary helper-free packaging cell line. *Nucleic Acids Res.*, **18**, 3587–3596.

Nardelli,B., Gonzalez,C.J., Schechter,M. and Valentine,F.T. (1995) CD4$^+$ blood lymphocytes are rapidly killed *in vitro* by contact with autologous human immunodeficiency virus-infected cells. *Proc. Natl Acad. Sci. USA*, **92**, 7312–7316.

Newton,K., Harris,A.W., Bath,M.L., Smith,K.G. and Strasser,A. (1998) A dominant interfering mutant of FADD/MORT1 enhances deletion of autoreactive thymocytes and inhibits proliferation of mature T lymphocytes. *EMBO J.*, **17**, 706–718.

Nguyen,H.L., Gruber,D. and Bulinski,J.C. (1999) Microtubule-associated protein 4 (MAP4) regulates assembly, protomer–polymer partitioning and synthesis of tubulin in cultured cells. *J Cell Sci.*, **112**, 1813–1824.

O'Connor,L., Strasser,A., O'Reilly,L.A., Hausmann,G., Adams,J.M., Cory,S. and Huang,D.C. (1998) Bim: a novel member of the Bcl-2 family that promotes apoptosis. *EMBO J.*, **17**, 384–395.

O'Keeffe,B., Fong,Y., Chen,D., Zhou,S. and Zhou,Q. (2000) Requirement for a kinase-specific chaperone pathway in the production of a Cdk9/cyclin T1 heterodimer responsible for P-TEFb-mediated Tat stimulation of HIV-1 transcription. *J. Biol. Chem.*, **275**, 279–287.

O'Reilly,L.A., Cullen,L., Visvader,J., Lindeman,G.J., Print,C., Bath,M.L., Huang,D.C. and Strasser,A. (2000) The proapoptotic BH3-only protein bim is expressed in hematopoietic, epithelial, neuronal and germ cells. *Am. J. Pathol.*, **157**, 449–461.

Ott,M., Emiliani,S., Van Lint,C., Herbein,G., Lovett,J., Chirmule,N., McCloskey,T., Pahwa,S. and Verdin,E. (1997) Immune hyperactivation of HIV-1-infected T cells mediated by Tat and the CD28 pathway. *Science*, **275**, 1481–1485.

Puthalakath,H., Huang,D.C., O'Reilly,L.A., King,S.M. and Strasser,A. (1999) The proapoptotic activity of the Bcl-2 family member Bim is regulated by interaction with the dynein motor complex. *Mol. Cell*, **3**, 287–296.

Rice,A.P. and Carlotti,F. (1990) Structural analysis of wild-type and mutant human immunodeficiency virus type 1 Tat proteins. *J. Virol.*, **64**, 6018–6026.

Roshal,M., Zhu,Y. and Planelles,V. (2001) Apoptosis in AIDS. *Apoptosis*, **6**, 103–116.

Sorger,P.K., Dobles,M., Tournebize,R. and Hyman,A.A. (1997) Coupling cell division and cell death to microtubule dynamics. *Curr. Opin. Cell Biol.*, **9**, 807–814.

Strasser,A., Harris,A.W., Huang,D.C., Krammer,P.H. and Cory,S. (1995) Bcl-2 and Fas/APO-1 regulate distinct pathways to lymphocyte apoptosis. *EMBO J.*, **14**, 6136–6147.

Wang,T.H., Wang,H.S. and Soong,Y.K. (2000) Paclitaxel-induced cell death: where the cell cycle and apoptosis come together. *Cancer*, **88**, 2619–2628.

Westendorp,M.O., Frank,R., Ochsenbauer,C., Stricker,K., Dhein,J., Walczak,H., Debatin,K.M. and Krammer,P.H. (1995) Sensitization of T cells to CD95-mediated apoptosis by HIV-1 Tat and gp120. *Nature*, **375**, 497–500.

Wolf,D., Witte,V., Laffert,B., Blume,K., Stromer,E., Trapp,S., d'Aloja,P., Schurmann,A. and Baur,A.S. (2001) HIV-1 Nef associated PAK and PI3-kinases stimulate Akt-independent Bad-phosphorylation to induce anti-apoptotic signals. *Nature Med.*, **7**, 1217–1224.

Zhang,J. and Winoto,A. (1996) A mouse Fas-associated protein with homology to the human Mort1/FADD protein is essential for Fas-induced apoptosis. *Mol. Cell. Biol.*, **16**, 2756–2763.

Received April 26, 2002; revised October 10, 2002; accepted October 29, 2002

Caspase cleavage of Bim_{EL} triggers a positive feedback amplification of apoptotic signaling

Dan Chen and Qiang Zhou*

Department of Molecular and Cell Biology, University of California, Berkeley, CA 94720-3202

Communicated by Randy Schekman, University of California, Berkeley, CA, December 4, 2003 (received for review November 4, 2003)

Members of the Bcl-2 protein family that share only the Bcl-2 homology 3 (BH3) domain are known mostly as sentinels for apoptotic stimuli and initiators of apoptosis. One BH3-only protein, Bim, is the major physiological antagonist of the prosurvival proteins in B and T lymphocytes. It is required for hematopoietic homeostasis and to preclude autoimmunity. Here, we show that the Bim_{EL} isoform, which was predominant in T cells, existed in both phosphorylated and unphosphorylated forms. Whereas the unphosphorylated Bim_{EL} was sequestered to microtubules by means of a direct interaction with tubulin, the phosphorylated protein was released from microtubules. The freed Bim_{EL} was subjected to caspase cleavage at an early stage of apoptosis induced by stimuli that activate either the mitochondria- or death receptor-dependent apoptosis pathway. The N-terminally cleaved Bim_{EL} became hyperactive in inducing apoptosis because of its more efficient targeting of Bcl-2. Thus, unlike many other BH3-only proteins, Bim_{EL} can be activated downstream of the caspase cascade, leading to a positive feedback amplification of apoptotic signals.

A key step in the mitochondria-dependent apoptotic pathway is the disruption of the mitochondria membrane. The integrity of the membrane is controlled primarily by a balance between the antagonistic actions of the proapoptotic and antiapoptotic members of the Bcl-2 family. The Bcl-2 homology 3 (BH3)-only family members constitute a key group of proapoptotic proteins that resemble Bcl-2 only in the BH3 domain. This domain is required for the interaction of these proteins with other Bcl-2 family members (1, 2). BH3-only proteins normally reside in other subcellular compartments or structures and translocate to the mitochondria in response to apoptotic stimuli. When at the mitochondria, they induce the conformational change and oligomerization of Bax and Bak, two Bcl-2 family members with BH1, BH2, and BH3 domains. The pore-forming capability of the oligomerized Bax and Bak results in the destabilization of the mitochondrial outer membrane and the subsequent release of the death molecules from the confines of the mitochondria (2). Antiapoptotic Bcl-2 family members, such as Bcl-2 and Bcl-xL, bind directly to the proapoptotic members, neutralize their activities, and abolish the apoptotic signaling. Given the pivotal role of the BH3-only proteins in sensing apoptotic stimuli and initiating apoptosis, their activities have to be kept in check to prevent inappropriate cell death (1).

Investigation into the diverse functions and regulations of the ≈10 known mammalian BH3-only proteins suggests that different proteins may initiate apoptosis in different cell types and/or transduce distinctive apoptotic stimuli in a given cell type (1, 3). Gene knock-out studies have revealed an essential role of one such protein, Bim, in shaping the development of the immune system and transducing the apoptotic signals caused by cytokine deprivation, calcium ion flux, and microtubule perturbation, but not other insults, in lymphocytes (4–7). Bim also facilitates HIV-1 Tat-induced apoptosis in T cells (8), which contributes in part to the progressive T cell depletion associated with AIDS.

Bim is the major physiological antagonist of the prosurvival proteins, at least in B and T lymphocytes (5). It is essential for the development of T cells (5) and apoptosis of activated T cells (7). Here, we report a previously undescribed mechanism by which Bim controls the apoptotic signaling in T cells. Three main isoforms of Bim (Bim_{EL}, Bim_L, and Bim_S) exist because of alternative splicing (9). The expressions of these isoforms vary in different cell types and tissues (10), with Bim_{EL} being the predominant one in T cells. Our data indicate that Bim_{EL} was sequestered to microtubules by means of a direct interaction with tubulin. Phosphorylated Bim_{EL} ($pBim_{EL}$) was released from microtubules and cleaved by caspases at an early stage of apoptosis, induced by stimuli that activate either the mitochondria- or the death receptor-dependent apoptotic pathway. The N-terminally cleaved Bim_{EL} demonstrated a higher affinity for Bcl-2 and a markedly enhanced apoptotic activity. The activation of Bim_{EL} downstream of the caspase cascade may provide a positive feedback amplification of apoptotic signals.

Methods

Cell Death Analyses. Apoptosis was induced in Jurkat T cells by 50 ng/ml tumor necrosis factor α (TNF-α)/0.5 μM staurosporine/0.05 μM taxol or by UV irradiation at a dose of 120 J/m^2. The broad-spectrum caspase inhibitor *N*-benzyloxycarbonyl-Val-Ala-Asp-fluoromethylketone was used at 20 μM. Cells were treated with 0.5 μM of the phosphatase inhibitor okadaic acid for 2 h. Cell death was measured by flow-cytometric analysis of hypodiploid nuclei stained with 20 μg/ml propidium iodide or annexin V–propidium iodide double stainin, according to the manufacturer's instructions (Roche Applied Science).

Phosphatase Treatment of Bim_{EL}. Jurkat T cells (1×10^6) were lysed in lysis buffer L containing 50 mM Hepes·KOH (pH 7.8), 150 mM NaCl, 5 mM EDTA, 0.5% Nonidet P-40, 2 mM DTT, and 0.5 mM PMSF. The lysate was dialyzed against 90 mM sodium citrate buffer (pH 4.8) containing 1 mM DTT, 1 mM PMSF, and the human protease inhibitor mixture (Sigma). After the addition of 1 unit of potato acid phosphatase (PAP; Sigma), the lysate was incubated at 30°C for 15 min and then analyzed.

Retroviral Infection and Cell Death Assay. Flag-tagged wild-type or truncated Bim_{EL} ($tBim_{EL}$) cloned into the pBabe-puro retroviral vector were transfected into the Phoenix retrovirus packaging cells (11, 12) with Lipofectamine-Plus reagent (Invitrogen). We mixed 1 ml of the viral supernatant with an equal volume of 1×10^6 per ml Jurkat cells 2 days later, and polybrene was added to a final concentration of 4 μg/ml. The infected Jurkat cells were selected with puromycin (0.5 μg/ml) in the media 2 days after infection. Viable puromycin-resistant cells were counted every 2 or 3 days during the subsequent 8-day period.

***In Vivo* and *in Vitro* Binding Assays.** For the *in vivo* Bcl-2-binding assay, constructs expressing the Flag-tagged wild-type or $tBim_{EL}$ were transfected into Jurkat T cells by electroporation. Cells

Abbreviations: BH, Bcl-2 homology; LC8, light chain 8; PAP, potato acid phosphatase; $pBim_{EL/L}$, phosphorylated $Bim_{EL/L}$; $tBim_{EL}$, truncated Bim_{EL}; TNF-α, tumor necrosis factor α.

*To whom correspondence should be addressed. E-mail: qzhou@uclink4.berkeley.edu.

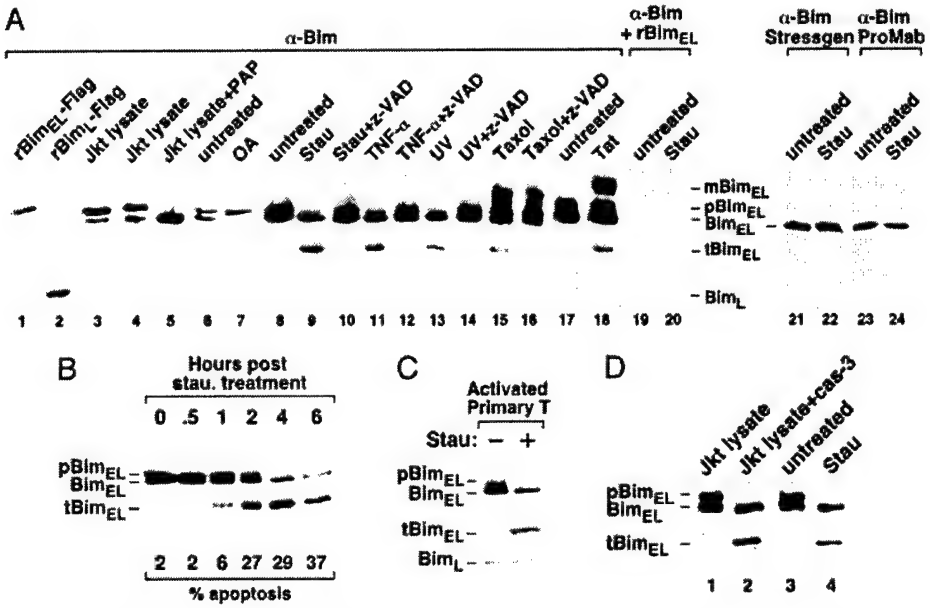

Fig. 1. Caspase cleavage of pBim$_{EL}$ in T cells at an early stage of apoptosis. (*A*) Caspase cleavage of pBim$_{EL}$ in apoptotic Jurkat T cells. Anti-Bim Western blotting was performed with the rabbit polyclonal antibodies directed against the full-length Bim$_{EL}$ to examine the purified Flag-tagged rBim$_{EL}$ and Flag-tagged rBim$_L$ (lanes 1 and 2), Jurkat cell lysates incubated with (lane 5) or without (lanes 3 and 4) PAP, and lysates from Jurkat cells subjected to the various treatments as indicated (lanes 7–20). In lanes 19 and 20, the antibody solution was preincubated with purified rBim$_{EL}$ before being used in Western blotting. In lanes 21–24, Western blotting was performed with anti-Bim antibodies obtained from StressGen Biotechnologies (Victoria, Canada) and ProMab Biotechnologies (Mountain View, CA), respectively. (*B*) Cleavage of pBim$_{EL}$ at an early stage of apoptosis. Lysates of Jurkat cells treated with staurosporine for the indicated periods of time (hr) were analyzed by anti-Bim Western blotting. The percentage of apoptotic cells was determined by flow-cytometric analysis and is indicated at the bottom. (*C*) Apoptosis-induced cleavage of pBim$_{EL}$ in activated mouse primary T cells. Anti-Bim Western blot analysis of lysates from activated mouse primary T cells treated with or without staurosporine. (*D*) pBim$_{EL}$ cleaved *in vitro* by recombinant caspases-3 comigrates with tBim$_{EL}$ from apoptotic Jurkat cells as indicated by anti-Bim Western blotting. Lanes 1 and 2, lysates from healthy Jurkat cells were incubated with or without recombinant caspase-3. Lanes 3 and 4 show lysates from Jurkat cells treated with or without staurosporine. Stau, staurosporine; OA, okadaic acid; mBim$_{EL}$, modified Bim$_{EL}$.

were lysed in the modified lysis buffer L, containing 500 mM NaCl, 2 days after transfection. Precleared lysate was incubated with the anti-Flag agarose beads (Sigma) at 4°C for 2 h. After extensive washes in the same buffer, Flag-tagged Bim$_{EL}$ and its associated Bcl-2 were eluted with the Flag peptide. The samples were subjected to Western blotting with anti-Bim and anti-Bcl-2 antibodies.

The *in vitro* tubulin-binding assay (8) was carried out by incubating 1 μg of purified tubulin (Sigma) with GST-Bim$_L$ or GST-Bim$_{EL}$ fusion proteins (1 μg) immobilized on glutathione agarose beads for 20 min at room temperature in 50 μl of binding buffer B (20 mM Tris, pH 7.5/500 mM NaCl/10% glycerol/0.2 mM EDTA/1 mM DTT/1 mM PMSF). After extensive washes with the same buffer, tubulin associated with GST-Bim$_L$ or GST-Bim$_{EL}$ was eluted with the SDS/PAGE sample buffer and detected by anti-tubulin Western blotting.

The microtubule-binding assay was performed essentially as described with some modifications (13). Jurkat cells (1×10^6) were lysed in lysis buffer L. The cleared lysate treated with or without PAP was incubated at 37°C for 20 min in the presence of 5 μg/ml taxol to reassemble microtubules. Apyrase was left out of the reaction to reduce the indirect docking of Bim onto microtubules through the motor proteins. The reaction mixture was subsequently loaded on top of a 40% sucrose cushion. Microtubules and their associated proteins were isolated by ultracentrifugation at 40,000 rpm for 20 min.

***In Vitro* Cleavage of Bim$_{EL}$.** *In vitro* cleavage of Bim$_{EL}$ in Jurkat cell lysate was carried out at 37°C for 4 h with recombinant caspase-3 (100 units; Calbiochem) by following the manufacturer's instructions. *In vitro* cleavage coupled with microtubule assembly was carried out by incubating the cleared Jurkat cell lysate (from 1×10^6 cells) with 5 μg/ml taxol at 37°C for 20 min. After microtubules were assembled, 100 units of recombinant caspase-3 (Calbiochem) were added. After a further incubation at 37°C for 4 h, the reaction mixture was subjected to ultracentrifugation.

Activated Mouse Primary T Cells. T cell suspensions from female C57BL/6 mice lymph nodes were cultured in RPMI medium supplemented with 10% FBS in plates coated with 5 μg/ml anti-CD3 and 1 μg/ml anti-CD28 for 2 h.

Results

Both Phosphorylated and Unphosphorylated Bim$_{EL}$ Exist in Jurkat T Cells. To elucidate the mechanism of Bim-controlled apoptosis in the immune system, the regulation of Bim activity during apoptosis in T cells was investigated. In Jurkat T cell lysate, Western blotting with the rabbit polyclonal antibodies directed against the full-length Bim$_{EL}$ (a generous gift from X. Luo and X. Wang, Howard Hughes Medical Institute and University of Texas Southwestern Medical Center, Dallas) revealed a doublet with mobility similar to that of the Flag-tagged recombinant Bim$_{EL}$ (rBim$_{EL}$) in an SDS gel (Fig. 1*A*, lanes 1 and 3). The antibodies did not detect the other two Bim isoforms (Bim$_L$ or Bim$_S$) in the lysate, although they are reactive with the rBim$_L$ and Bim$_S$ proteins (lane 2 and data not shown). Because phosphorylation often controls the activity of the Bcl-2 family members (14), we suspected that the doublet detected by immunoblotting might represent the phosphorylated and unphosphorylated forms of Bim$_{EL}$. In support of this idea, incubation of Jurkat cell lysate with PAP converted the upper band of the doublet into the lower one (Fig. 1*A*, lanes 4 and 5). In contrast, treatment of Jurkat cells with the phosphatase inhibitor okadaic acid produced the opposite effect of turning the lower band into the

upper one (lanes 6 and 7). Thus, the upper band most likely contained the $pBim_{EL}$.

Caspase Cleavage of $pBim_{EL}$ at an Early Stage of Apoptosis. Interestingly, treatment of Jurkat cells with several apoptosis stimuli, such as the cytotoxic drug staurosporine, UV irradiation, and the death-inducing cytokine TNF-α, resulted in the disappearance of the upper band and the appearance of a new faster-migrating band of ≈22 kDa (Fig. 1*A*, lanes 9, 11, and 13). This effect was completely blocked by *N*-benzyloxycarbonyl-Val-Ala-Asp-fluoromethylketone (lanes 10, 12, and 14), a broad-spectrum caspase inhibitor, suggesting that the ≈22-kDa fragment was probably a caspase-cleaved product of $pBim_{EL}$ ($tBim_{EL}$). To confirm the specificity of the polyclonal antibodies used in immunoblotting, the antibody solution was preincubated with the purified $rBim_{EL}$ before its incubation with the membrane. This process completely abrogated the detection of both the doublet and the ≈22-kDa fragment (Fig. 1*A*, lanes 19 and 20), indicating that these proteins indeed originated from Bim_{EL}. It is worth noting that the anti-Bim antibodies purchased from StressGen Biotechnologies and ProMab Biotechnologies detected neither the $pBim_{EL}$ nor the cleaved $tBim_{EL}$ (Fig. 1*A*, lanes 21–24).

A time-course analysis revealed that $tBim_{EL}$ began to appear in Jurkat T cells 1 h after the treatment with staurosporine, at which time only ≈6% cells were undergoing apoptosis (Fig. 1*B*). The caspase cleavage of Bim_{EL} at an early stage of apoptosis suggested that $tBim_{EL}$ was not merely an end product generated in dead cells but, rather, may contribute to the execution and progression of apoptosis from the beginning.

Different from staurosporine, UV, and TNF-α, both the microtubule-perturbation drug taxol and the HIV-1 Tat protein, which was shown recently to induce apoptosis by disrupting microtubule dynamics (8), caused not only the caspase-dependent cleavage but also a caspase-independent modification of Bim_{EL}. This finding was illustrated by the appearance of a slow-moving Bim_{EL} species in the gel ($mBim_{EL}$; Fig. 1*A*, lanes 15, 16, and 18). The nature and significance of this modification remain to be investigated. We suspect that it may be responsible for the observed strong dependence on Bim for both taxol- and Tat-induced apoptosis in T cells (5, 8).

Finally, it is important to point out that the caspase cleavage of the $pBim_{EL}$ was not restricted to Jurkat T cell line. Induction of apoptosis in activated mouse primary T cells by staurosporine also caused the cleavage of the $pBim_{EL}$ (Fig. 1*C*).

***In Vitro* Cleavage of $pBim_{EL}$ by Recombinant Caspase-3.** Because the apoptotic stimuli activating either the mitochondria pathway (staurosporine, UV, taxol, and Tat) or the death receptor pathway (TNF-α) were all capable of inducing the cleavage of $pBim_{EL}$, the downstream effector caspases that are common to both pathways were probably responsible for this effect. Consistent with this idea, incubation of recombinant caspases-3 (Calbiochem) with the lysate of healthy Jurkat cells yielded a cleaved $pBim_{EL}$ fragment that comigrated with the $tBim_{EL}$ generated *in vivo* from apoptotic Jurkat cells (Fig. 1*D*). This finding further confirmed the 22-kDa fragment as a caspase-cleaved product of $pBim_{EL}$.

Caspase Cleavage of Bim_{EL} After Asp-13. To determine the cleavage site in Bim_{EL}, a series of N- and C-terminal deletion mutants of Bim_{EL} with truncations after several candidate Asp residues were produced and their mobility in an SDS gel was compared with that of the proteolytic fragment of $pBim_{EL}$ from apoptotic cells (Fig. 2*A*). Deletion of the first 7 or the last 21 amino acids from Bim_{EL} produced protein fragments that migrated slower than the caspase-cleaved 22-kDa $tBim_{EL}$. $tBim_{EL}$, however, comigrated with the N-terminal deletion mutant $Bim_{EL}\Delta N13$

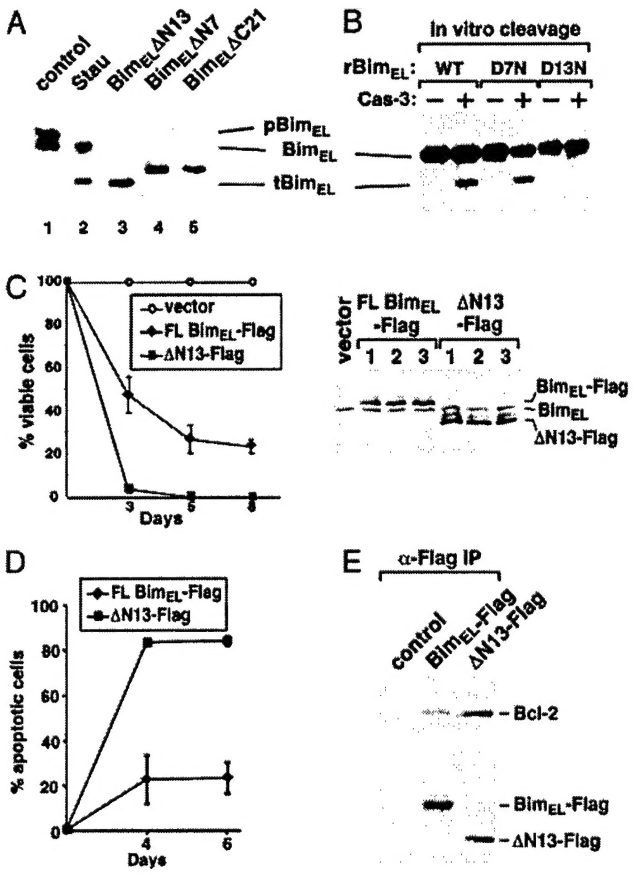

Fig. 2. N-terminal cleavage of Bim_{EL} after Asp-13 enhances its interaction with Bcl-2 and induction of apoptosis. (*A*) *In vivo* caspase-cleaved $tBim_{EL}$ comigrates with $rBim_{EL}\Delta N13$ in SDS gel. Bim_{EL} truncated after the various Asp residues were expressed in transfected 293T cells. Their mobility was compared with that of $tBim_{EL}$ from staurosporine (Stau)-treated Jurkat cells by Western blotting. (*B*) Mutation of Asp-13 to Asn in Bim_{EL} prevents cleavage by caspase-3. Anti-Bim Western blot analysis of recombinant wild-type (WT) and mutant (D7N and D13N) Bim_{EL} before (−) or after (+) the incubation with recombinant caspase-3. (*C*) Expression of ΔN13 greatly reduces cell survival. Jurkat cells infected with retroviruses expressing full-length Flag-tagged Bim_{EL} (FL Bim_{EL}-Flag), Flag-tagged ΔN13 (ΔN13-Flag), or nothing (vector) were selected with puromycin at 2 days after infection. The percentage of surviving cells was determined over the subsequent 8 days, and the average from three independent infections is shown (*Left*). Flag-tagged Bim_{EL} and Flag-tagged ΔN13 produced in Phoenix retrovirus packaging cells from three independent transfections were analyzed by anti-Bim Western blotting, which also detected the endogenous Bim_{EL} (*Right*). (*D*) ΔN13 has greater apoptotic activity than wild-type Bim_{EL}. Plasmids expressing Flag-tagged Bim_{EL} or Flag-tagged ΔN13 were electroporated into Jurkat cells. Apoptosis was measured by flow-cytometric analysis of annexin V-positive and propidium iodide-negative cells. (*E*) ΔN13 binds more Bcl-2 than Flag-tagged Bim_{EL} or control. Flag-tagged Bim_{EL}, Flag-tagged ΔN13, and their associated Bcl-2 were immunoprecipitated (α-Flag IP) from the lysates of transfected Jurkat cells and analyzed by Western blotting as indicated.

lacking amino acids 2–13 (Fig. 2*A*, lanes 2 and 3). Further deletion to the next Asp at position 53 or 157 produced much smaller Bim_{EL} fragments (data not shown). Further support for the existence in Bim_{EL} of a caspase-cleavage site after Asp-13 came from the observation that mutation of Asp-13 to Asn (D13N) in $rBim_{EL}$ abolished its cleavage by caspase-3 *in vitro*, whereas mutation of Asp-7 to Asn (D7N) had no effect (Fig. 2*B*).

Cleaved Bim_{EL} Has Greater Apoptotic Activity. Bim_{EL} has been identified as an apoptosis inducer. However, its potency is

significantly lower than that of the other two alternatively spliced isoforms, Bim_L and Bim_S (9). We next investigated whether the proapoptotic activity of Bim_{EL} could be enhanced by the removal of the 13 amino acids at its N terminus. Phoenix retrovirus packaging cells (11) were transfected with the empty pBabe-puro vector (12) or pBabe-puro expressing full-length Bim_{EL} or ΔN13. The produced viruses were then used to infect Jurkat T cells and the surviving puromycin-resistant cells were counted over a period of 8 days. With the survival rate of cells infected with the empty vector set at 100%, sustained expression of both full-length Bim_{EL} and Bim_{EL}ΔN13 reduced the number of surviving cells. However, when the infection efficiency was adjusted to about the same level as reflected by the expression of the two Bim_{EL} proteins in the packaging cells (Fig. 2*C Right*), ΔN13 was found to be much more efficient in reducing the number of viable cells than the full-length Bim_{EL} (Fig. 2*C Left*). Detection of apoptotic cells by annexin V–propidium iodide double staining (Roche) revealed that ΔN13 produced from the transfected plasmids caused significantly more apoptosis than did the full-length Bim_{EL} (Fig. 2*D*). Thus, the proapoptotic activity of Bim_{EL} can be enhanced by the cleavage of the 13 amino acids at its N terminus.

Cleaved Bim_{EL} Binds More Efficiently to Bcl-2. Bim has been shown to induce apoptosis by interacting with the prosurvival Bcl-2 family members through its BH3 region (9). Because ΔN13 demonstrated higher apoptotic activity than the full-length Bim_{EL}, we examined whether this was because of its increased binding to Bcl-2. Constructs expressing the Flag-tagged full-length Bim_{EL} and ΔN13 were electroporated into Jurkat T cells, and Bcl-2 associated with the immunoprecipitated Bim_{EL} proteins was analyzed by Western blotting. When the expressions of Bim_{EL} and ΔN13 were normalized to a similar level, the amount of Bcl-2 associated with ΔN13 was significantly higher than that with the full-length Bim_{EL} (Fig. 2*E*). Thus, the N terminus of Bim_{EL} appeared to have an inhibitory effect on the Bim_{EL}–Bcl-2 interaction. The removal of the N-terminal 13 residues may expose the BH3 region for a more efficient binding to Bcl-2.

Direct Interactions of Tubulin and Microtubules with Bim_{EL} but Not Bim_L. We asked how, if only the $pBim_{EL}$ could undergo caspase cleavage during apoptosis, the phosphorylation of Bim_{EL} might control this process. The observation that the bacteria-produced $rBim_{EL}$, which presumably was unphosphorylated, could be cleaved by caspase-3 *in vitro* (Fig. 2*B*) suggests that the Bim_{EL} phosphorylation was not essential for the cleavage process *per se*. This observation raises a possibility that the phosphorylation may release Bim_{EL} from a certain kind of sequestration, making Bim_{EL} accessible to caspase cleavage.

What sequesters the unphosphorylated Bim_{EL} and protects it from caspase cleavage? Bim_{EL} and Bim_L have been shown to interact with the dynein light chain 8 (LC8), which is part of the microtubular dynein motor complex (13). Apoptotic stimuli provoked the release of Bim_L and LC8, allowing Bim_L to associate with Bcl-2-like proteins (13). Although Bim_{EL} and Bim_L interact with LC8 (13) and Bcl-2 (9) with similar efficiency, Bim_L is much more apoptotic than Bim_{EL} (9). It is possible that Bim_{EL} is sequestered to microtubules more tightly than Bim_L by means of additional interactions, which may prevent its migration to the mitochondria.

In support of this hypothesis, purified tubulin (Sigma) was found to interact directly with immobilized GST-Bim_{EL} but not GST-Bim_L (Fig. 3*A*). An *in vivo* interaction of tubulin with Flag-tagged Bim_{EL}, but not Flag-tagged Bim_L, was also detected in anti-Flag immunoprecipitates derived from transfected 293T cells (Fig. 3*B*). These data indicate that Bim_{EL} bound directly to tubulin through a region (amino acids 42–97) that is missing from Bim_L.

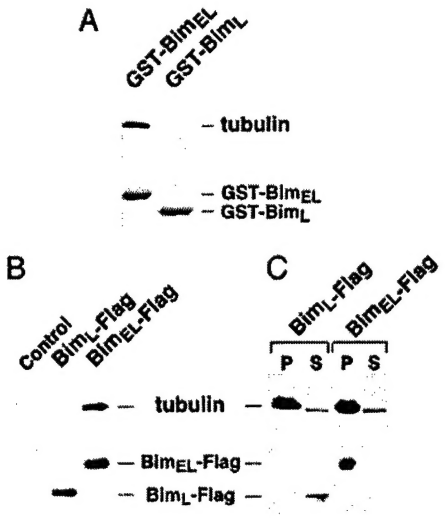

Fig. 3. Bim_{EL} is sequestered to microtubules by means of its direct interaction with tubulin. (*A*) Bim_{EL}, but not Bim_L, binds directly to tubulin *in vitro*. Immobilized GST-Bim_{EL} and GST-Bim_L were incubated with purified tubulin. The Bim-associated tubulin was detected by anti-α-tubulin Western blotting. (*B*) Bim_{EL}, but not Bim_L, binds to tubulin *in vivo*. Anti-Flag immunoprecipitates from lysates of 293T cells transfected with Flag-tagged Bim_{EL} (Bim_{EL}-Flag) or Bim_L (Bim_L-Flag) were subjected to Western blotting to detect the Bim-associated tubulin. (*C*) Bim_{EL}, but not Bim_L, binds to polymerized microtubules. Cleared lysates of 293T cells transfected with Flag-tagged Bim_{EL} or Flag-tagged Bim_L were incubated with taxol and then subjected to ultracentrifugation. The levels of α-tubulin and Bim in the pellet (P) and the supernatant (S) were determined by Western blotting.

To determine whether Bim_{EL} could also bind to polymerized microtubules, we performed a microtubule assembly assay in 293T cell lysate containing the transfected Flag-tagged Bim_{EL} or Flag-tagged Bim_L. The modified assembly conditions (see *Methods*) reduced the binding of motor proteins to microtubules and, as a result, the indirect docking of Bim onto microtubules through the motors. On ultracentrifugation to separate the polymerized microtubules and their associated proteins from the rest of the cell lysate, Bim_{EL}, but not Bim_L, was found to associate with microtubules (Fig. 3*C*).

$pBim_{EL}$ Escapes Sequestration by Microtubules. Microtubule-associated proteins (MAPs) interact with the negatively charged tubulin tails through their positively charged tubulin-binding regions. Phosphorylation of MAPs disrupts these interactions (15). We next asked whether, like other MAPs, $pBim_{EL}$ could dissociate from microtubules, leading to its cleavage by caspases. First, microtubule-stabilizing drug taxol was added to cleared Jurkat cell lysate pretreated with or without PAP, or to cell lysate prepared from Jurkat cells treated with or without the phosphatase inhibitor okadaic acid. Ultracentrifugation was then performed to separate polymerized microtubules and their associated Bim_{EL} in the pellet from free tubulin and other soluble proteins in the supernatant. Both fractions, as well as the sample, were analyzed by Western blotting before ultracentrifugation (Fig. 4*A*, T). Without the PAP treatment, the majority of the unphosphorylated Bim_{EL} remained bound to microtubules in the pellet, whereas all of the $pBim_{EL}$ resided in the supernatant. After the PAP treatment, unphosphorylated Bim_{EL} migrated from the supernatant to the pellet to associate with the polymerized microtubules. In contrast to PAP, okadaic acid converted the unphosphorylated Bim_{EL} to the phosphorylated form, which dissociated from microtubules and stayed in the supernatant. Together, these two complementary approaches

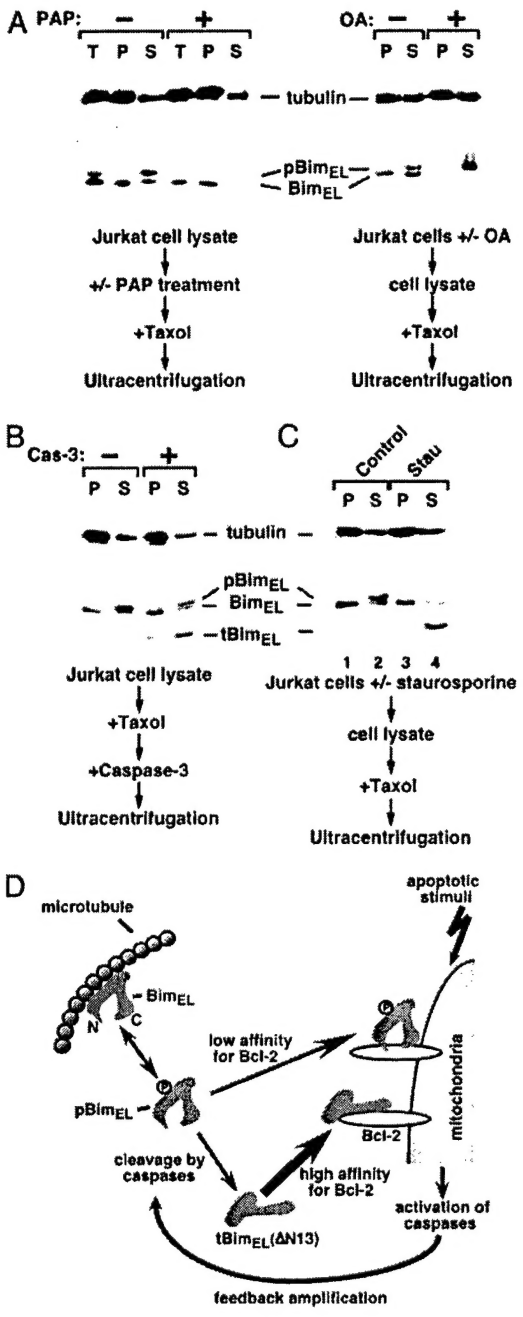

Fig. 4. pBim$_{EL}$ escapes sequestration by microtubules and becomes accessible to caspase cleavage. (*A*) pBim$_{EL}$ is released from microtubules. Jurkat cell lysate preincubated with or without PAP (*Left*) or lysate from Jurkat cells treated with or without okadaic acid (*Right*) was incubated with taxol and then subjected to ultracentrifugation. α-Tubulin and Bim in the pellet (P), supernatant (S), or lysate before centrifugation (T) were detected by Western blotting. (*B*) The association with microtubules prevents Bim$_{EL}$ from cleavage by caspase-3 *in vitro*. Jurkat cell lysate was incubated with taxol to assemble microtubules. Recombinant caspase-3 was then added to the reaction. After ultracentrifugation, α-tubulin and Bim were analyzed as in *A*. (*C*) pBim$_{EL}$ is released from microtubules and cleaved by caspases in apoptotic Jurkat cells. Lysate from Jurkat cells treated with or without staurosporine (Stau) was subjected to the same analysis as in *A*. (*D*) Diagram depicting the activation of a positive feedback apoptotic pathway involving the release of pBim$_{EL}$ from microtubules and caspase cleavage of pBim$_{EL}$. The cleaved tBim$_{EL}$(ΔN13) binds more Bcl-2 and has greater apoptotic activity. tBim$_{EL}$ may or may not contain the phosphorylation sites, which have not been mapped in the full-length Bim$_{EL}$. See the text for details.

revealed a preference of microtubules to bind to the unphosphorylated Bim$_{EL}$.

pBim$_{EL}$ Is Much More Accessible to Caspase Cleavage. To determine whether the phosphorylation-mediated release of Bim$_{EL}$ from microtubules would lead to an enhanced caspase cleavage of this protein, we first compared the efficiency of cleavage between the free and the microtubule-bound Bim$_{EL}$ by recombinant caspase-3 *in vitro* (Fig. 4*B*). After the assembly of microtubules in Jurkat cell lysate, caspase-3 was incubated with the mixture. The reaction was then subjected to ultracentrifugation to separate microtubules from free tubulin. Compared with only a weak cleavage of the microtubule-bound, unphosphorylated Bim$_{EL}$, a much more efficient cleavage of the free pBim$_{EL}$ was observed (Fig. 4*B*). This conclusion was supported further by the result obtained in staurosporine-treated Jurkat cells, in which only the pBim$_{EL}$ released from microtubules was cleaved (Fig. 4*C*).

Discussion

Bim is the major physiological antagonist of the prosurvival proteins in B and T lymphocytes (5). It functions by maintaining hematopoietic homeostasis and precluding autoimmunity (5). By performing experiments in Jurkat and activated mouse primary T cells, in which expression of the Bim$_{EL}$ isoform is predominant, we have discovered a mechanism by which Bim$_{EL}$ participates in the control of apoptosis (Fig. 4*D*). Bim$_{EL}$ was found to exist in both the phosphorylated and unphosphorylated forms in healthy cells, and the unphosphorylated form was sequestered to microtubules by means of a direct interaction with tubulin. This interaction depended on a region in Bim$_{EL}$ that is missing in Bim$_L$, allowing Bim$_{EL}$ to be more tightly sequestered to microtubules and, consequently, less available for Bcl-2 binding than Bim$_L$. This finding may explain why Bim$_{EL}$ is generally less apoptotic than Bim$_L$ (9), despite the fact that both can bind to the dynein LC8 (13) and Bcl-2 (9) with similar efficiency.

Phosphorylation of Bim$_{EL}$ caused it to dissociate from microtubules. The freed Bim$_{EL}$, however, was mostly inactive because it displayed a low affinity for Bcl-2 (Fig. 4*D*). On the induction of apoptosis, the pBim$_{EL}$ released from microtubules was processed by a caspase(s) to generate an N-terminally truncated fragment (ΔN13) with an increased affinity for Bcl-2 and a significantly enhanced apoptotic activity. Because apoptotic stimuli activating either the death receptor pathway (TNF-α) or the mitochondria pathway (UV, staurosporine, Taxol, and HIV-1 Tat) are all capable of inducing the cleavage of Bim$_{EL}$, it is likely that a caspase(s) that is common to both pathways is responsible for this event. Although caspase-3 has been shown to cleave Bim$_{EL}$ *in vitro*, it is important to point out that the caspase(s) that is in charge *in vivo* remains to be elucidated.

What could the caspase cleavage of Bim$_{EL}$ contribute to the overall control of apoptosis in T cells? Several pieces of data suggest that the cleavage is not required for the initiation of apoptosis. First of all, the induction of apoptosis did not cause any enhancement in Bim$_{EL}$ phosphorylation (as reflected by similar levels of unphosphorylated Bim$_{EL}$ in healthy and apoptotic cells; Fig. 4*C*) or release of Bim$_{EL}$ from microtubules (Fig. 4*C*, compare lanes 1 and 3). More importantly, the cleavage of Bim$_{EL}$ depended on the activation of the downstream caspases. Although the cleavage of Bim$_{EL}$ does not trigger the onset of apoptosis, it may in fact contribute to a positive feedback amplification of apoptotic signals (Fig. 4D). This idea is supported by the demonstration that the cleaved tBim$_{EL}$ occurred very early during the course of apoptosis and was unlikely to be a simple end product generated in dead cells (Fig. 1*B*). Furthermore, tBim$_{EL}$ was more active than the full-length protein in targeting Bcl-2 and inducing apoptosis (Fig. 2). It is worth noting that this signal-amplification mechanism initiated by the cleav-

age of Bim_{EL} seems to apply only to mature T cells, whereas in immature T cells undergoing apoptosis, an increased expression of Bim_{EL} and Bim_L has been observed (6). It is unclear what causes such a change in Bim_{EL} regulation and whether this change is biologically significant for T cell development.

It is interesting to note that although the signal-amplification effect caused by caspase cleavage of the $pBim_{EL}$ is different from the reported role of the Bim_L isoform in sensing and initiating the apoptosis pathway (13), similarities can be detected in the control of the activities of the two isoforms. In human breast carcinoma cell line MCF-7 and mouse IL-3-dependent promyelocytic cell line FDC-P1, certain apoptotic stimuli can lead to the phosphorylation of Bim_L by the Jun N-terminal kinase (16) and the subsequent release of Bim_L from the sequestration by the microtubular dynein motor complex. This process enables Bim_L to translocate to the mitochondria and target Bcl-2 or its homologues to initiate apoptosis (13).

The signal-amplification function of the caspase-cleaved Bim_{EL} is similar to a previously described amplification activity displayed by another BH3-only protein Bid. Induction of death receptor-initiated apoptosis triggers the activation of caspase-8, which cleaves the inactive cytosolic form of Bid into a truncated Bid (tBid). tBid then translocates to mitochondria and displays higher affinity for antiapoptotic Bcl-2 (17, 18). Whereas the Bid-mediated amplification may be more restricted to the death receptor pathway, Bim_{EL} appears to function in a more general manner to amplify death signals initiated from both the mitochondria- and the death receptor-pathways. Future experiments are needed to shed more light on the posttranslational regulation of Bim_{EL} and the biological consequences of the Bim_{EL}-mediated signal-amplification process.

We thank Drs. X. Wang and X. Luo for the anti-Bim antibodies. We also thank Drs. A. Strasser, J. Allison, A. Winoto, K. Luo, and their laboratories for valuable reagents, technical help, and expert advice. This work was supported by grants from the National Institutes of Health (AI-41757), the American Cancer Society (RSG-01-171-01-MBC to Q.Z.), and the U.S. Army Breast Cancer Predoctoral Fellowship (DAMD17-02-1-0321 to D.C.).

1. Puthalakath, H. & Strasser, A. (2002) *Cell Death Differ.* **9,** 505–512.
2. Wang, X. (2001) *Genes Dev.* **15,** 2922–2933.
3. Huang, D. C. & Strasser, A. (2000) *Cell* **103,** 839–842.
4. Bouillet, P., Cory, S., Zhang, L. C., Strasser, A. & Adams, J. M. (2001) *Dev. Cell* **1,** 645–653.
5. Bouillet, P., Metcalf, D., Huang, D. C., Tarlinton, D. M., Kay, T. W., Köntgen, F., Adams, J. M. & Strasser, A. (1999) *Science* **286,** 1735–1738.
6. Bouillet, P., Purton, J. F., Godfrey, D. I., Zhang, L. C., Coultas, L., Puthalakath, H., Pellegrini, M., Cory, S., Adams, J. M. & Strasser, A. (2002) *Nature* **415,** 922–926.
7. Hildeman, D. A., Zhu, Y., Mitchell, T. C., Bouillet, P., Strasser, A., Kappler, J. & Marrack, P. (2002) *Immunity* **16,** 759–767.
8. Chen, D., Wang, M., Zhou, S. & Zhou, Q. (2002) *EMBO J.* **21,** 6801–6810.
9. O'Connor, L., Strasser, A., O'Reilly, L. A., Hausmann, G., Adams, J. M., Cory, S. & Huang, D. C. (1998) *EMBO J.* **17,** 384–395.
10. O'Reilly, L. A., Cullen, L., Visvader, J., Lindeman, G. J., Print, C., Bath, M. L., Huang, D. C. & Strasser, A. (2000) *Am. J. Pathol.* **157,** 449–461.
11. Grignani, F., Kinsella, T., Mencarelli, A., Valtieri, M., Riganelli, D., Lanfrancone, L., Peschle, C., Nolan, G. P. & Pelicci, P. G. (1998) *Cancer Res.* **58,** 14–19.
12. Morgenstern, J. P. & Land, H. (1990) *Nucleic Acids Res.* **18,** 3587–3596.
13. Puthalakath, H., Huang, D. C., O'Reilly, L. A., King, S. M. & Strasser, A. (1999) *Mol. Cell* **3,** 287–296.
14. Strasser, A., O'Connor, L. & Dixit, V. M. (2000) *Annu. Rev. Biochem.* **69,** 217–245.
15. Lee, G. (1993) *Curr. Opin. Cell Biol.* **5,** 88–94.
16. Lei, K. & Davis, R. J. (2003) *Proc. Natl. Acad. Sci. USA* **100,** 2432–2437.
17. Luo, X., Budihardjo, I., Zou, H., Slaughter, C. & Wang, X. (1998) *Cell* **94,** 481–490.
18. Li, H., Zhu, H., Xu, C. J. & Yuan, J. (1998) *Cell* **94,** 491–501.